

CHARACTERIZING THE ROLE OF DNA POLYMERASE GAMMA IN THE YEAST,
CRYPTOCOCCUS NEOFORMANS

A thesis presented to the faculty of the Graduate School of Western Carolina University in
partial fulfillment of the requirements for the degree of Master of Science in Biology

By

Joshua Ellis Boggs

Director: Dr. Indrani Bose
Associate Professor of Biology
Biology Department

Committee Members: Dr. Jamie Wallen, Chemistry
Dr. Robert Youker, Biology

Thesis Reader: Dr. Heather Coan, Biology

November 2017

TABLE OF CONTENTS

LIST OF TABLES	iv
LIST OF FIGURES	v
LIST OF TERMS/ABBREVIATIONS	vii
LIST OF ABBREVIATED GENES	viii
ABSTRACT	ix
Chapter I. INTRODUCTION	1
A. The discovery, life cycle, and significance of <i>Cryptococcus neoformans</i>	1
B. The discovery, function, and significance of Mitochondria	6
C. The discovery, function, and significance of DNA Polymerase Gamma (DNA polG)	8
Chapter II. MATERIALS AND METHODS	14
A. Strains Used	14
B. Media and Growth Conditions	14
C. Identification of the MIP1 Gene sequence within <i>Cryptococcus neoformans</i>	15
D. Genomic DNA Preparation	15
E. Making the MIP1 RNAi (MIP1i) plasmid	16
i. pIBB103 plasmid	16
ii. Cloning exonic portion of MIP1 into the pIBB103 RNAi vector using SLIC	17
iii. Cloning the MIP1 exon into pIBB103 using T4 DNA Ligase	18
F. Making the MIP1-mCherry NEO ^R plasmid	19
G. Making the CTR4p-MIP1-mCherry (NEO ^R) plasmid	22
H. Making the pGPDp-MIP1-GFP plasmid	24
I. Transforming <i>C. neoformans</i> by electroporation	25
i. Electroporation of JEC21 cells with the pIBB103-MIP1 (MIP1i) construct	25
ii. Electroporation of KN99 mata α cells with the pLK25-MIP1 or pLK25-CTR4p-MIP1 constructs	26
J. Biolistic Transformation	26
K. Growth Curves	27
i. Determination of effective 5-FOA levels in growth curves	27
L. Mitotracker TM Green live cell assay	27
M. Deconvolution of Mitotracker stained images	28
N. Primers Used	29
Chapter III. RESULTS	30
A. Identifying <i>C. neoformans</i> MIP1 gene by sequence homology	30
B. Determining the essentiality of DNA polymerase gamma in <i>C. neoformans</i> by RNA interference	33
C. Growth of cells when MIP1 gene product is decreased	35
i. Growth of cells within YPD-NEO or YPG-NEO containing 1mg/ml 5-FOA	35
ii. Growth of cells within YPD-NEO or YPG-NEO containing 0.2mg/ml 5-FOA	37
D. Effect of MIP1p depletion on mitochondrial stability	39
i. Development of the mitochondrial stability assay	40
ii. Mitochondrial stability is decreased in cells grown on YPGal-NEO plates	41
iii. Growing cells from YPD-NEO that were previously not induced for RNAi	42
E. Efforts to localize fluorescently tagged DNA polymerase gamma	44

F. CnMIP1 expressed from a regulatable promoter	46
Chapter IV. Discussion	49
A. Identifying the <i>C. neoformans</i> MIP1 gene by sequence homology	49
B. Determining the essentiality of DNA polymerase gamma to the survival of <i>C. neoformans</i> ..	50
C. Mitochondrial staining of cells in the absence of MIP1	51
D. Localization of Mip1p.....	52
E. Future Directions	54
i. Localizing MIP1 using <i>C. neoformans</i> codon optimized mEGFP	54
ii. Replacement of the endogenous promoter with the CTR4 copper inducible promoter within the genome of <i>C. neoformans</i>	54
iii. Activity of CnpolG and study of its domains	56
REFERENCES	57
APPENDIX.....	66

LIST OF TABLES

Table 1: Primers used in this project.....	38
--	----

LIST OF FIGURES

Figure 1. pIBB103 vector used for MIP1 RNAi.....	17
Figure 2. pLK25 vector used for MIP1 localization.....	20
Figure 3. Amino acid BLAST search comparing the <i>C. neoformans</i> genome against the <i>S. cerevisiae</i> DNA polG sequence.....	31
Figure 4. Presence of conserved domains within the DNA polymerase gamma homolog found within <i>C. neoformans</i>	32
Figure 5. Domain alignment of DNA polG amino acid sequences from human (top), <i>S. cerevisiae</i> (middle), and <i>C. neoformans</i> (bottom). This alignment was created using domain predictions from the National Center of Biotechnology Information’s online BLAST database.....	32
Figure 6. (a) Structure of pIBB103-mip1 plasmid. (b) SpeI digest of pIBB103-mip1 transformants. (1- 4 are plasmid digests from four pIBB103-mip1 colonies; L=1kb Generuler DNA ladder).....	34
Figure 7. Replica plate of pIBB103-mip1 (top) and pIBB103-empty (bottom) from YPG-NEO onto YPG-NEO containing 5-FOA.....	35
Figure 8. OD600 readings of cells containing either the pIBB103-mip1 construct, or the pIBB103 construct. Time points (in hours) of sample collection are indicated. Broken lines indicate presence of YPG-NEO media, solid lines indicate presence of YPD-NEO media. 1mg/ml 5-FOA was added to all YPG-NEO cultures at the 3h time point. [Standard deviation used for error bars].....	36
Figure 9. OD600 readings of cells containing either the pIBB103-mip1 construct, or the pIBB103 construct. Cells containing either construct were grown for 24 hours in levels of 5-FOA that varied from 0, 0.125, 0.25, or 0.5mg/ml 5-FOA, as indicated in the figure legend. 5-FOA was added at the 3h time point for in all cultures. [Standard deviation used for error bars].....	38
Figure 10. OD600 readings of cells containing either the pIBB103-mip1 construct, or the pIBB103 construct. Time points (in hours) of sample collection are indicated. Broken lines indicate presence of YPG-NEO media, solid lines indicate presence of YPD-NEO media. 0.2mg/ml 5-FOA was added to all YPG-NEO cultures at the 3h time point. [Standard deviation used for error bars].....	39
Figure 11. (a) Wild type JEC21 cell stained with 0.2µM Mitotracker™ Green live cell dye for 30 minutes. (b) Wild type JEC21 cells stained with 0.2µM Mitotracker™ Green for 30 minutes. Scale bar is equal to 20µm.....	41
Figure 12. (a) Average levels of fluorescence emitted by cells containing either the pIBB103-mip1 construct, or the pIBB103 construct. Presence of 5-FOA within solution is indicated above. (b) Flow chart briefly describing the experiment shown in Figure 12(a). [Standard deviation used for error bars].....	42
Figure 13. (a) Levels of fluorescence emitted by cells containing either the pIBB103-mip1 construct, or the pIBB103 construct. Presence of 5-FOA within solution is indicated above. (b) Flow chart briefly describing the experiment carried out to produce the graph shown in figure 13(a). [Standard deviation used for error bars].....	43
Figure 14. (a) Product of PCR reaction carried out in order to amplify the MIP1 gene along with the genes endogenous promoter from KN99α genomic DNA. (- indicates the negative control within the reaction. + indicates the PCR reaction containing MIP1 along with 562bp	

of upstream DNA). (b) Restriction digest of plasmid DNA using XbaI that contains MIP1 cloned within the pJET 1.2 cloning vector. The product of two bands that are 2793bp and 5075bp, confirms that MIP1 was successfully cloned into the vector.....	45
Figure 15. MIP1 first exon PCR amplification using plasmid DNA from 6 colonies transformed by the pLK25-MIP1 ligation reaction. The numbers 1-6 correspond to the colony from which the PCR template originated. The - corresponds to the negative control in the PCR. L contains an NEB 1kb ladder.	45
Figure 16. Results of restriction digest carried out on plasmid DNA from 10 colonies potentially transformed with the pLK25-CTR4p construct using the restriction enzyme AvrII. A single linear band in transformants 1-3 indicates that the CTR4p fragment is found within the vector.....	47
Figure 17. PCR confirmation of the presence of MIP1 within the pLK25-CTR4p construct. A band present at 4513bp shows a positive result, indicating that MIP1 is in fact present within the construct. - indicates the negative control within the reaction.	48
Figure 18. RNA seq data from multiple laboratories showing the production of mRNA from the CnMIP1 gene. This data was collected from FungiDB.com. Black arrows indicate introns within the CnMIP1 gene.	55
A1. Figure 19. Protein alignment of <i>S. cerevisiae</i> polG and <i>C. neoformans</i> polG homolog.....	68
A2. Figure 20. Protein alignment of JEC21 (Serotype D) (top) and H99 (Serotype A) (bottom) <i>C. neoformans</i> DNA polymerase gamma.....	71

LIST OF TERMS/ABBREVIATIONS

ddNTP	Dideoxynucleotide
gDNA	Genomic DNA
KN99 <i>matα</i>	Serotype A Strain
JEC21	Serotype D Strain
JEC43	<i>ura5</i> mutant (Serotype D)
DTT	Dithiothreitol
PBS	Phosphate Buffered Saline
YPD	Yeast Extract, Peptone, Dextrose
YPG	Yeast Extract, Peptone, Galactose
LB	Lysogeny Broth
SDS	Sodium Dodecyl Sulfate
BCS	Bathocuproine disulfonic acid
ATP	Adenosine triphosphate
NADPH	Nicotinamide adenine dinucleotide phosphate
G418	Geneticin

LIST OF ABBREVIATED GENES

<i>MIP1</i>	DNA polymerase Gamma gene
<i>CTR4</i>	Copper Transporter 4 gene
GFP	Green fluorescent protein
mCherry	Monomeric Cherry
<i>URA5</i>	Orotidine 5' phosphate decarboxylase gene
PrimPol	Primase polymerase

ABSTRACT

CHARACTERIZING THE ROLE OF DNA POLYMERASE GAMMA IN THE YEAST, *CRYPTOCOCCUS NEOFORMANS*

Joshua Ellis Boggs, Master of Science in Biology

Western Carolina University (November 7, 2017)

Director: Indrani Bose

The basidiomycetous yeast, *Cryptococcus neoformans*, is an opportunistic pathogen that is responsible for a common fungal infection of the central nervous system, cryptococcal meningoencephalitis. This is a signal disease of AIDs patients that can also be found in patients of other immune compromising afflictions. This disease can be treated with various antifungal medications, but these drugs must be taken in combination, and are often far too expensive for widespread availability. The current shortcomings of available treatments make it critical that we understand vital systems within this organism that may lead to development of more effective and potentially cheaper medications. DNA polymerase gamma (polG or Mip1p) has been identified as the only polymerase in yeast that is capable of replication and repair of the entire mitochondrial (mt) genome. In *S. cerevisiae*, deletion of DNA polG leads to the overall lack of mtDNA and the production of *petite* or *wee* colonies. *C. neoformans* is known to be aerobic, and therefore, the integrity of its mitochondrial DNA is hypothesized to be vital to the survival of the yeast. This necessity of mtDNA replication and maintenance makes polG a strong candidate as a potential drug target. Using amino acid sequence homology, a *MIP1* homolog has been identified in *C. neoformans*. This gene, CNAG_06769, has a 45% identity to the *MIP1* gene in *S. cerevisiae* and contains a mitochondrial localization signal (MLS) as well as a DNA polymerase

A domain, which is found in all known DNA polG proteins. The polymerase domain identified in *C. neoformans* polG contains a 62% identity and a 76% similarity to the same domain found in *S. cerevisiae* polG. There are also regions within the cryptococcal protein that have previously not been seen in other fungal or mammalian polG proteins. This has raised questions regarding what the functions of these domains may be and how these functions may be relevant in DNA polG research. In this project, RNAi has been used to silence the *MIP1* gene (*MIP1i*). Galactose-dependent knock-down of Cn*MIP1* shows that this gene appears to be essential to *C. neoformans* survival. Growth curves of the *MIP1i* strains compared to those of wild type cells show that the strains are unable to proliferate in the absence of this protein. In addition, mitochondrial integrity assays using the vital dye Mitotracker Green indicate that RNAi of *MIP1* affects the viability of these cells. Localization of the CnpolG protein with a C-terminal mCherry tag was also attempted. Constructs were created to express this protein from its endogenous promoter, as well as from a copper-repressible promoter. However, the attempts to localize this protein *in vivo* have been inconclusive to date and require further optimization.

CHAPTER I. INTRODUCTION

A. The Discovery, Life Cycle, and Significance of *Cryptococcus neoformans*

The kingdom Fungi are a diverse group of interesting organisms that is divided into seven separate phyla. The two largest groups of this kingdom are put together into the subkingdom Dikarya, which is often referred to as the higher fungi. These two groups are known as the Basidiomycetes and the Ascomycetes. Basidiomycetes include groups such as mushrooms, puffballs, stinkhorns and, mirror yeasts.¹ Organisms of this group are filamentous fungi that form specialized reproductive cells called basidiospores. These cells form at the end of reproductive structures called basidia. During reproduction, basidiospores are often forcibly ejected from the basidia allowing for these spores to disperse. Ascomycetes, which are more commonly known as the sac fungi, are a large group of fungi that are defined by the presence of an ascus in which ascospores are formed. Some members of this group include truffles, and the widely-used organism commonly known as baker's yeast (*S. cerevisiae*).¹

Cryptococcus neoformans is a basidiomycetous yeast that is identified as being within the class Tremellomycetes. This yeast is a single celled organism that replicates via budding, but under the correct mating conditions, is capable of producing hyphae with basidiospores at the end of its reproductive structures.² *C. neoformans* is an opportunistic human pathogenic fungus that can be commonly found in the soil throughout the world,³ even within the mountains of western North Carolina. It is responsible for the disease cryptococcal meningoencephalitis, which is commonly associated with HIV/AIDS infected patients.⁴ This association occurs because the patient's immune system is greatly suppressed by the viral infection, which allows the yeast to successfully evade host immunity, survive, grow, and cause disease. As of 2015, approximately 40 million people throughout the world were living with HIV/AIDS, and cryptococcal meningitis

was the most common fungal infection found within the central nervous system of these patients.⁵ Cryptococcal infections have also been identified in patients not afflicted with HIV/AIDS, but these cases are incredibly rare and involve other immune compromising conditions, such as Non-Hodgkin's lymphoma, Hodgkin's lymphoma, and organ transplants.⁶

C. neoformans was first discovered by the German pathologist Otto Busse and the surgeon Abraham Buschke in 1894.⁷ When the yeast was first isolated from an infection within a lesion found on the tibia of a young woman, these men described it as a *Saccharomyces*-like organism.⁷ Later that year, the scientist Francesco Sanfelice isolated this same organism from a fermenting peach.⁸ He demonstrated that this yeast was pathogenic in lab animals. Eventually it was determined that this organism did not produce ascospores as believed when initially discovered; this prevented the organism from being classified as a *Saccharomyces*.⁹ The initial discovery of *C. neoformans* in a human patient showed that the yeast was fully capable of infecting human hosts, under the correct conditions. It is now well established that this yeast can readily infect humans with immune system suppression.

Over time, *C. neoformans* has been called by many different names. It was first called *Saccharomyces hominis* by the German scientist Busse in 1894.⁷ Later Buschke reviewed this organism and the tibial infection in which it was found and determined that it was a *coccidium*.⁷ Next in 1895, Sanfelice named this organism *Saccharomyces neoformans*. In 1896, the French pathologist Curtis described a yeast infection found within the groin of a man that led to a central nervous system infection, and named the yeast *Megalococcus myxoides*. After further testing Curtis changed the name of his organism to *Saccharomyces subcutaneous tumefaciens*. In 1901, Vuillemin renamed the organisms that were isolated by Busse and Curtis as *Cryptococcus hominis*, while he renamed Sanfelice's isolate as *Cryptococcus neoformans*. This name change

was carried out most importantly in order to distinguish these organisms from the ascospore-forming *Saccharomyces*.

Cryptococcus neoformans has now been classified in two separate species, *C. neoformans* (Serotypes A and D) and *C. gattii* (Serotypes B and C). The four separate serotype classifications are based on antigenic differences that were discovered to be present in each. These antigenic differences were discovered to be based on differing structural compositions of the major capsule polysaccharide, glucuronoxylomannan.¹³ In addition, the different serotypes can be separated by the use of biochemical studies,¹⁰ morphological differences within the perfect state of the serotypes,¹¹ and by their genetic characteristics.¹² In fact, genetic differences were used to further separate *C. neoformans* into two separate varieties, *C. neoformans* var. *grubii* (Serotype A) and *C. neoformans* var. *neoformans* (Serotype D). The distribution of serotype A and serotype D isolates are different from one another, with serotype A being most commonly found in most of the world except for northern Europe. Serotype D isolates are most often found in temperate climates and are found most often in infections of the skin.¹⁴ Serotype D strains are also shown to be more susceptible to heat than serotype A cells, which could possibly explain why the organism is not found more commonly throughout the globe.¹⁵

C. neoformans contains a number of distinct virulence factors that allow this organism to infect mammals and to also evade host defenses organisms, such as humans or mice. The presence of a polysaccharide capsule has long been shown to be directly associated with virulence in this organism.¹⁶ This capsule is composed of long polymers of α -1,3-mannan with monosaccharide branches of xylose and glucuronic acid.¹⁷ The most current thinking is that this polysaccharide capsule exists in order to protect the organism from desiccation in nature, and to

reduce the ability of the organism to be ingested and destroyed by soil inhabiting phagocytic amoeba, which could be encountered in the yeast's normal environment.¹⁸

The first gene that was identified as being critical to the production of the capsule in *C. neoformans* was called *CAP59*. This gene was identified using random UV mutagenesis and was discovered to no longer produce a viable capsule.¹⁹ This result was confirmed by using homologous recombination to delete *CAP59*. The $\Delta cap59$ strains showed an acapsular phenotype with dry, wrinkled colonies. Soon after its establishment, the acapsular phenotype was directly associated with loss of virulence in murine models. This loss of virulence indicated that the capsule was needed for survival and virulence in the mammalian host; a conclusion that was supported when complementation of *CAP59* restored virulence in mice.¹⁹

There are a number of effects that the capsule has on the host that have been shown to contribute to the virulence of the organism. A few of these effects include anti-phagocytosis,²⁰ complement depletion,²¹ antibody unresponsiveness,²² high negative charge of cells,²³ and inhibition of leukocyte migration.²⁴ Combined, all of these factors add up to protect *C. neoformans* from host immunity within humans and other mammals.

Melanin synthesis is another important virulence factor for *C. neoformans*' successful host infection. The ability to produce the pigment melanin is unique to *C. neoformans* in the *Cryptococcus* genus. It is thought that synthesis of melanin using the phenol oxidase enzyme, otherwise known as laccase, may have evolved due to the niche that *C. neoformans* holds in nature, in which the yeast decays phenolic compounds found within the wood of various trees.²⁵ The laccase enzyme is able to metabolize catechol precursors to produce the pigment melanin. Two laccase enzymes are encoded within the nuclear genome of *C. neoformans*.²⁶ The *LAC1* gene encodes a laccase that is the primary producer of cellular melanin, while the *LAC2* gene

encodes a secondary laccase that appears to play a small role in melanin production.²⁷ This has been shown experimentally by the introduction of mutations within *LAC1* showing none to very little cellular melanin production.²⁸ Deletions of the *LAC2* gene, on the other hand, have no discernable effect on cellular melanin production.²⁸ Some compounds that can be used as substrates for this pathway include epinephrine, nor-epinephrine, L-DOPA, and dopamine. The structure of the melanin pigment in *C. neoformans* is not well understood, but the presence of the pigment is believed to assist in virulence in a number of separate but important ways. These include antioxidant activity,²⁹ cell wall integrity,³⁰ cell wall charge,³¹ protection from high temperature by potential dissipation of heat energy,³² and reduction to the effectiveness of some common antifungal agents.³³

Other virulence factors associated with *C. neoformans* include urease production, phospholipase production, as well as the ability to grow at 37°C. Urease is a nickel metallo-enzyme that catalyzes the hydrolysis of urea to ammonia and carbamate. This enzyme allows the yeast to respond to pH changes, allowing for survival in seemingly harsh conditions.³⁴ Along with harsh pH condition adaptation, the ability to maintain life and to replicate at high temperature is another very important factor for the yeast to overcome in order to be capable of growing and replicating within a mammalian host.³⁵

It was originally discovered that drugs that inhibited the calmodulin-activated serine/threonine-specific phosphatase, known as calcineurin had no effect on *C. neoformans* at 24°C but killed the yeast at 37°C.³⁵ This indicated that calcineurin played a large role in the heat tolerance of the organism, and without the use of this pathway the organism could not survive at elevated temperatures.³⁵ High temperatures have been shown to reduce transcription of genes involved in nucleotide and amino acid biosynthesis.³⁵ There are genes that are specifically

induced by the change of temperature within *C. neoformans*; some of these include trehalose synthase, catalase, and superoxide dismutase.³⁶

B. The Discovery, Function, and Significance of Mitochondria

Intracellular structures that resembled what are now known as mitochondria were first discovered in the 1840's. This dates the discovery of mitochondria only a few years after the discovery of the nucleus, which was found in 1833.³⁷ In 1890, Altmann was the first individual to realize that mitochondria were present ubiquitously in the cells of more than one organism,³⁸ suggesting that these organelles were very important to the function of many types of cells. He termed these structures "bioblasts". Before the theory of the endosymbiotic origins for mitochondria was widely accepted throughout the scientific community, Altmann was convinced that mitochondria were "elementary organisms" living within the cell. It is quite interesting to realize that Altmann was most likely on the right track with his ideas on how mitochondria may have originated. He was convinced that these bioblast's carried out vital functions within the cell. In 1898, an alternative name for these organelles was suggested. The name "mitochondria" was proposed because of the organelle's appearance³⁹; it comes from the Greek words "mitos" (meaning thread), and "chondros" (meaning granules).

The first discoveries of mitochondrial function were made by Michaelis in 1900, when he found that the redox dye Janus Green B functions as a live cell stain for mitochondria.⁴⁰ Nearly half a century later it was shown that the staining of mitochondria by this dye is due to the mitochondria's capacity to oxidize the reduced dye by utilizing the enzyme cytochrome oxidase.⁴¹ Up to this point, any proposed function of mitochondria was based entirely off of observation and not experimentation. Friedrich Meves and Claude Regaud, both scientists involved in early mitochondrial research, suggested that the role of mitochondria within the cell

could be to “bear genes”.^{42,43} This was not an entirely incorrect idea, since it has been found that mitochondria do, in fact, contain their own DNA that is separate from nuclear DNA in the cell. The confirmation that mitochondria carry out chemical reactions that were most likely essential to the organism, opened the door to further research of this organelle.

In the 1930’s groundbreaking discoveries led to a great leap in the available knowledge about mitochondria. In 1937, Hans Krebs presented his idea of the citric acid cycle in the journal *Nature*.⁴⁴ This was a very important discovery that brought Krebs much esteem throughout his life, and this cycle is now often called the Krebs cycle in his honor. Soon after, Herman Kalckar made some initial discoveries into the pathway of aerobic respiration.⁴⁵ Early work such as these studies were later built onto to determine the true function of mitochondria.

Mitochondria are now known to be the powerhouse of the cell. This is due to their now well-studied role of using simple resources such as glucose to form energy supplies, such as ATP and NADH, that can be readily used by the cell. This is carried out within the mitochondria by the citric acid cycle and the electron transport chain. Glycolysis is a separate function of the cell that takes place within the cytoplasm. Utilizing all of these systems cells can generate, on average, 38 molecules of ATP can be generated by a single glucose molecule by aerobic respiration - 2 molecules of ATP are generated by glycolysis, 2 molecules of ATP are generated by the Krebs cycle, and 34 molecules of ATP are generated by the electron transport chain.^{46,47,48} Some energy is lost throughout this process due to the leakiness of the system. The role of mitochondria as an energy producer within the cell makes this organelle very important for survival and growth, especially within aerobic organisms. Some organisms such as *S. cerevisiae* are able to survive on fermentable media without functional mitochondria, but these cells form petite colonies that are smaller than the average wild type cell. Other aerobic organisms, such as

humans, cannot survive without functioning mitochondria within the cells. Only anaerobic organisms are capable of survival without mitochondria.

Mitochondria contain their own unique genome (mtDNA). Mitochondrial DNA in human's codes for 13 protein products, 22 tRNA's and 2 rRNA's.⁴⁹ All of the protein products that are coded for by the mitochondria, are involved in the oxidative phosphorylation process.⁵⁰ Due to the importance of each aspect of the mtDNA, it is critical that the cell have the means for its synthesis and maintenance. Both of these functions are carried out by the protein, DNA polymerase Gamma.⁵¹

C. The Discovery, Function, and Significance of DNA Polymerase Gamma (DNA polG)

DNA polymerase gamma is the only known polymerase to function in the mitochondria that is capable of mtDNA replication, proofreading, and maintenance in animals and fungi. It was first discovered in 1970 as a polymerase activity isolated from higher eukaryotes, and from *S. cerevisiae* mitochondria that showed aphidicolin-resistance and high sensitivity to ddNTP's.⁵²⁵³ Mitochondrial fractions taken from the cells of various organisms were used to test for polymerase function, and showed a single corresponding activity. DNA polymerase gamma has been most highly studied in humans due to the enzymes role in various human diseases. DNA polG was believed to be the only mitochondrial DNA polymerase present within human cells, until the discovery of Primase polymerase (PrimPol).⁵⁴ PrimPol is shown to assist in repriming of DNA synthesis on stalled replication forks. This function leads to better genomic stability within cells.

DNA polymerase gamma has also been well-studied in *S. cerevisiae* because it can survive without the presence of active mitochondria, which is fatal in many eukaryotes. *S. cerevisiae* colonies devoid of mitochondria, or containing damaged mitochondria, can grow on

media that allows for fermentation producing smaller colonies, often referred to as “petite” colonies.⁵⁵ In *S. cerevisiae*, the absence of the nuclear gene, *MIP1*, that codes for DNA polG, leads to a lack of mitochondrial DNA and ultimately, to a lack of mitochondria.⁵⁵ Cells devoid of mitochondria are no longer able to carry out aerobic respiration, and in many organisms this lack of aerobic respiration is fatal. Mutations in this protein have been shown to greatly affect the stability of mtDNA in other eukaryotic organisms, such as humans.⁵⁶ Due to the nuclear origin of the *MIP1* gene, this sequence contains a mitochondrial localization signal in order to enter the mitochondria where its function is carried out.

The gene that codes for DNA polG, *MIP1*, was discovered in a genetic screen for temperature sensitive mutants of *S. cerevisiae* that were able to grow on glycerol at 25°C, but not at 36°C.⁵⁵ It was shown to lack all mitochondrial DNA replication, as well as mitochondrial DNA polymerase activity, suggesting that the gene in question was possibly responsible for the polymerase activity in the mitochondria.⁵⁵ *MIP1* was located within the genome of *S. cerevisiae* and was identified as being present on chromosome 15, and coded for a protein that was 1254 amino acids in length.⁵¹ Once *MIP1* was identified and cloned, the gene was deleted in yeast to determine the knockout phenotype. As expected, the resulting mutants were completely lacking in mitochondrial DNA.⁵⁶

After this enzyme’s function was established, the next step was to determine what domains were present in the protein and what they were used for in the cell’s mitochondrial replication and repair. The DNA polG in *S. cerevisiae* has been shown to contain an MLS (mitochondrial localization signal), a N-terminus domain, an exonuclease domain, a spacer domain, a polymerase domain, and a C-terminal tail.⁵⁷ These domains have also been shown to be present in the protein in other organisms, such as humans.⁵⁷ Each domain is believed to play a

specific role in the synthesis and housekeeping function of the enzyme. The possession of both a polymerase domain, as well as an exonuclease domain, suggested this enzyme was fully capable of not only DNA synthesis, but also DNA proofreading and DNA maintenance.

The polymerase domain in DNA polG is responsible for the actual synthesis of mtDNA. This domain has been shown to contain three subdomains known as the thumb, palm, and the fingers. The function of this region has been studied experimentally by creating three mutations in the finger subdomain. These mutations resulted in increases in point mutations as well as increased extended mutability.⁵⁹ This experiment showed that the catalytic domain of the enzyme is involved in DNA polymerization as well as fidelity.

The polymerase domain, when compared to various bacterial DNA polymerases, has been shown to belong to the class A family of polymerases. It is highly conserved throughout many species such as *Homo sapiens*, *S. cerevisiae*, *Xenopus laevis*, and *Rattus norvegicus*.^{60, 61, 62, 63} Differences in this region do exist between the various species that may lead to processivity differences within each enzyme.

When the catalytic domain of DNA polG was first purified, an active exonuclease domain co-purified with it, indicating that both the polymerase domain as well as the exonuclease domain were found in a single polypeptide.⁵ The exonuclease domain of the enzyme is directly responsible for the proofreading capabilities it exhibits. Using alignments to bacterial DNA polymerases, three well conserved exonuclease motifs were found in this exonuclease domain. Single mutations were carried out in each sub-domain in order to determine the associated phenotypes.⁶⁴ The mutations greatly decreased the effectiveness of the proofreading capabilities of the DNA polG enzyme.⁶⁴ Soon after, a mouse model completely lacking in polG exonuclease activity was created.⁶⁵ This exonuclease devoid DNA polG had astounding effects

on the mice. Errors within the mtDNA of the mice increased, early onset aging was observed as the lifespan of the mice was decreased.⁶⁵ This suggests that exonuclease function is vital to prevent premature aging.

The spacer region in between the polymerase and exonuclease domains (Figure 5) is hypothesized to be directly involved in the proper folding of the enzyme, as well as the binding site for accessory subunits.⁶⁶ In the human DNA polG dimeric accessory subunits bind to the catalytic subunit of the enzyme,⁶⁷ in *Drosophila melanogaster* the accessory subunit is monomeric, in *S. cerevisiae* an accessory protein is not present.^{68,69} This suggests that *S. cerevisiae* carries out the function of this accessory subunit using other methods. The spacer region of the enzyme, although not catalytically functional itself, is known to be responsible for disease when mutated in the human enzyme.⁵⁷ The specific mutation G737R, has been linked to Alpers, Myocerebrohepatopathy and other Infantile syndromes caused by mtDNA depletion.⁵⁷

The C-terminal tail of DNA polymerase gamma varies greatly in length between species. It is directly involved in the polymerization of DNA strands and appears to play a role in strand displacement during DNA synthesis within *S. cerevisiae*.⁵⁸ In *S. cerevisiae*, the presence of the longer, and functional C-terminal tail may prevent the enzyme from requiring the accessory subunits that are required in other species. This is predicted because this domain functions as a DNA helicase during DNA synthesis.⁶⁸ Experimentally this has been shown by the deletion of the last 216 residues of the domain. Many of the residues in this region are highly conserved, and when they are deleted the mutability of the polymerase function of the enzyme increases dramatically.⁵⁸ The deletion of the same 216 amino acids appears to have no effect on exonuclease activity of the enzyme.⁵⁸ In the presence of low concentrations of dNTP's the strand displacement function of the enzyme appears to be reduced approximately by half.⁷⁰ In *C.*

neoformans a much shorter C-terminal tail is present (Figure 5) , this indicates that accessory subunits are most likely required for DNA synthesis in this organism, as in humans.

Several accessory proteins are directly involved in the replication, and repair that is carried out by DNA polG. These include, mitochondrial single stranded binding protein, mitochondrial helicase, RNase H1, topoisomerases, DNA ligase III, and other proteins and transcription factors.⁷¹ The mitochondrial single stranded binding protein (mtSSB) has been shown to enhance helix destabilization for the associated DNA helicases, and polG.⁷² This function directly supports mitochondrial DNA replication, and repair *in vivo*. In *D. melanogaster*, the presence of mtSSB has been shown to increase mitochondrial DNA synthesis by around 40-fold.⁷³ Mutations in this protein have also been shown to cause significant decreases in mitochondrial DNA synthesis.⁷²

The ATP dependent mitochondrial helicase *TWINKLE*, has been shown to be directly involved in mtDNA maintenance and regulation of the amount of total mitochondrial DNA present within mammals.⁷⁴ *TWINKLE* colocalizes with mtDNA *in vivo*, and contains a 5' to 3' helicase domain. Overexpression of *TWINKLE* in murine models has shown an increase in overall mtDNA copy numbers present within a cell, while a reduction in *TWINKLE* lowers the amount of mtDNA present.⁷⁴ These studies suggest that *TWINKLE* plays a significant role in the maintenance of copy numbers of mitochondrial DNA that are present within each cell.

Certain RNase's, as well as topoisomerases are also present in mitochondrial DNA synthesis and repair within the cell.⁷¹ RNase H1 is a cellular RNase that is found in high copy numbers within the nucleus, but is also found in much lower numbers to be present in the mitochondria. It is hypothesized that this enzyme plays a role in mtDNA synthesis by the removal of RNA primers during DNA replication.⁷⁵ Topoisomerases such as Topo I and

TopoIII α have been shown to be present in the mitochondria. These enzymes are believed to relax and remove supercoils that are present due to the activity of the mitochondrial helicase.⁷⁶

In this project, I have identified the DNA polymerase gamma encoding gene in *C. neoformans*, *CnMIP1*. The polG product encoded for by *CnMIP1* is highly conserved to the polG found in *S. cerevisiae* and humans, although it has novel domains that are unique to the *C. neoformans* protein (see Discussion). I have shown that this gene is essential to the survival of *Cryptococcus neoformans* and have tried to localize the protein in the cell.

CHAPTER II. MATERIALS AND METHODS

A. Strains Used

The KN99 mat α (Serotype A) strain was used for all of the mCherry localization experiments. The Neomycin resistance gene (NEO^R) is found within the construct in order to select for transformed colonies.

The JEC21 (Serotype D) strain was used for all RNAi experiments as both the source material for genomic inserts of targeted genes and for the RNAi vector transformations and growth assays.

The JEC43 (*ura5*) strain was used for GFP construct expression using *URA5* as a selectable marker. This strain is unable to synthesize the essential amino acid uracil.

B. Media and Growth Conditions

All *C. neoformans* strains were maintained in YPD media (1% yeast extract, 2% tryptone, and 2% dextrose) at 30°C. For selection of specific transformants, YPD media was supplemented with the antifungal drug neomycin (Geneticin or G418, Fisher BioReagents #BP673) at 100 μ g/ml.

Media that is lacking the amino acid uracil was used for selection of transformation colonies that contained the *URA5* selectable marker. This media was made using a –uracil dropout mix (US Biological) that contains all of the essential amino acids except for uracil.

All biolistic transformations were carried out on YPD plates containing 1M sorbitol before transferring to the appropriate selective medium for growth.

Bacterial cultures were grown in LB broth media (0.5% yeast extract, 1% tryptone, and 1% NaCl). Agar plates containing LB media supplemented with 100 μ g/mL ampicillin or

kanamycin were used as appropriate for selection of cells containing the desired plasmid constructs. SOC media (2% vegetable peptone, 0.5% yeast extract, 10mM NaCl, 2.5mM KCl, 10mM MgCl₂, 10mM MgSO₄, 20mM Glucose; NewEngland BioLabs INC. #B9020S) was used for outgrowth during bacterial transformations.

Cells were tested for RNAi on YPG (1% yeast extract, 2% tryptone, and 2% galactose) media supplemented with the drug Geneticin with and without 5-fluoroorotic acid (5-FOA) at 1mg/ml on plates, and 1mg/ml or 0.2mg/ml in liquid media.

C. Identification of the *MIP1* Gene Sequence within *Cryptococcus neoformans*

The identification of the sequence of the *MIP1* sequence in *Cryptococcus neoformans* was carried out utilizing the online genomic sequence database FungiDB (FungiDB.org).

Protein sequence comparisons were carried out between DNA polymerase Gamma of humans, *S. cerevisiae*, and *C. neoformans*, using the online software Clustal Omega(<https://www.ebi.ac.uk/Tools/msa/clustalo/>).

D. Genomic DNA Preparation

Genomic DNA was prepared using the method described by Bose et al.⁷⁶ Briefly, 3mls of cells were grown overnight in YPD media at 30°C and were harvested by centrifugation at ~12,000g. The cells were lysed in 0.5ml extraction buffer (50mM Tris-HCL, pH 8; 20mM EDTA; 1% SDS) by bead beating the cells using a vortex mixer or bead beater on high speed for 2 minute intervals, letting the cells rest on ice for 1 minute in between. This process was repeated until approximately 50-80% breakage was obtained, as determined by light microscopy. The samples were then incubated at 70°C for 10 minutes, vortexed well, and treated with 200µl 5M potassium acetate and 150µl 5M NaCl. Samples were mixed by inversion, incubated on ice for 20 minutes, and then centrifuged at 14,500rpm for 20 minutes. Supernatant from each sample

was transferred to a clean tube. 450µl chloroform was added and the samples were centrifuged for 10 minutes at 14,500 rpm. The aqueous phase was transferred to a new tube with 200µl of PEG 8000. Samples were incubated on ice for 10 minutes, before being centrifuged for 10 minutes. Supernatant was removed from each sample and discarded. Each pellet was re-suspended in 50µl sterile water. The supernatant from the samples were treated with 1µl 500µg/ml RNase and incubated at 37°C for 30 minutes to remove RNA from the samples. A 1/10th volume of 3M sodium acetate (5µl), and 3 volumes of ethanol (150µl) were added to each sample. Samples placed in -20°C for 30 minutes, and centrifuged at 14,500rpm for 10 minutes at 4°C. The supernatant was removed from each sample and the pellet was resuspended in 50µl sterile water.

E. Making the *MIP1* RNAi (*MIP1i*) plasmid

i. pIBB103 plasmid

The pIBB103 RNAi vector (see Figure 1) was used for making the *MIP1i* (*MIP1 RNAi*) construct. The plasmid contains a bacterial origin of replication, an ampicillin^R gene for selection in bacteria, and a NEO^R gene for selection in yeast on the drug G418. This plasmid has an RNAi cassette that contains two *GAL7* promoters coding in opposite directions that are flanked by terminators, functionally creating dsRNA when active. Between the promoters, a *ura5* segment is present for *URA5* RNAi, which assists with 5-FOA selection.

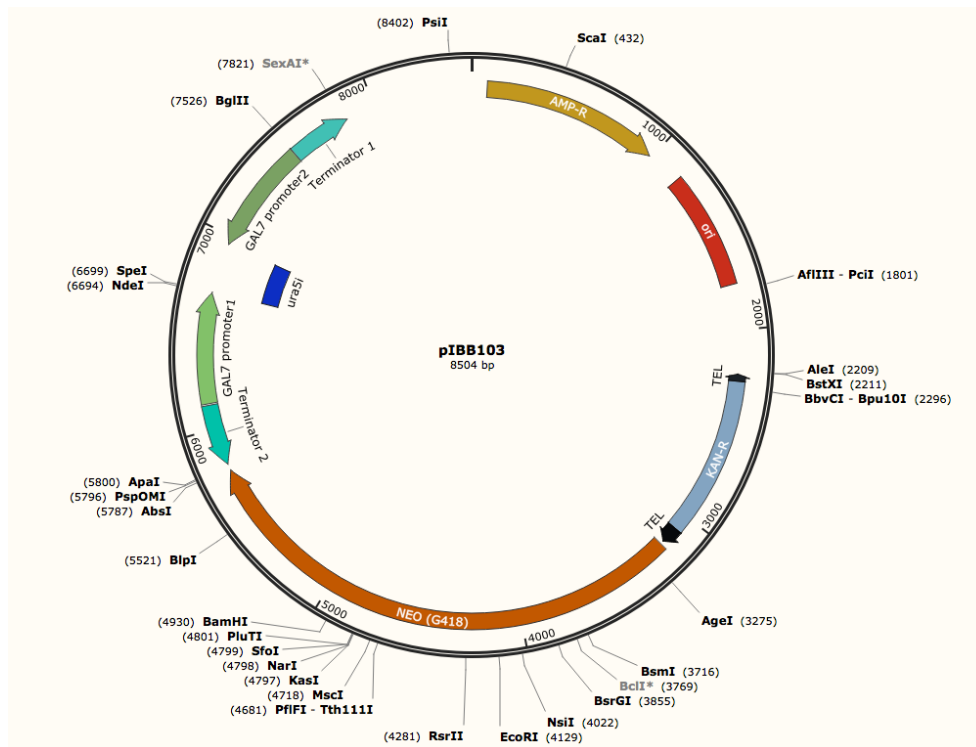


Figure 1. pIBB103 vector used for *MIP1* RNAi.

ii. Cloning exonic portion of *MIP1* into the pIBB103 RNAi vector using SLIC

A PCR reaction was carried out to amplify bases 697-956 of the *MIP1* gene that is part of the third exon. This reaction was performed using BLO163 as the forward primer, BLO164 as the reverse primer (see Table 1), and genomic DNA from JEC21 (Serotype D) as the template. The reaction mix for this PCR reaction contained 1 μ l template DNA, 5 μ l Q5 reaction buffer, 0.5 μ l dNTP's, 1.5 μ l 10 μ M BLO163, 1.5 μ l 10 μ M BLO164, 0.75 μ l DMSO, 0.3 μ l Q5[®] High-Fidelity polymerase, and 14.5 μ l water. The reaction conditions used were 98 $^{\circ}$ C 30s; 30 x (98 $^{\circ}$ C 10s, 57 $^{\circ}$ C 30s, 72 $^{\circ}$ C 2:30m); 72 $^{\circ}$ C 2m. The PCR product obtained from this reaction was column purified. The pIBB103 plasmid (see Figure 1.) was linearized with SpeI, incubated at 37 $^{\circ}$ C for 5h. The SpeI digest contained 15 μ l pIBB103 plasmid DNA, 6 μ l 10xCutsmart[™] buffer, 32 μ l water, and 2 μ l SpeI restriction enzyme in a total reaction volume

of 60 μ l. The linearized pIBB103 from the SpeI digest was column purified using the Wizard® SV Gel and PCR Clean-up System (Promega) following the manufacturer instruction, and resuspended in 50 μ l of water.

A SLIC,⁷⁸ (Sequence and Ligation Independent Cloning) cloning reaction was set up in order to place the *mip1* insert within pIBB103. The SLIC reaction contained 1 μ l NEB buffer 2, 1 μ l SpeI-digested pIBB103 DNA, 1 μ l or 0 μ l *mip1* DNA, in a final volume of 10 μ l with water. These SLIC reactions were incubated with 0.25 μ l T4 DNA polymerase added and reacted for 20 minutes at room temperature. Ligation was carried out by endogenous *E. coli* repair enzymes. Transformation was carried out with 2.5 μ l SLIC reactions into 50 μ l of competent *E. coli* and plated onto LB plates containing 100 μ g/ml ampicillin.

iii. Cloning the *MIP1* exon into pIBB103 using T4 DNA Ligase

Due to the failure of SLIC cloning, the PCR amplified *mip1* fragment from E (ii) was cloned into the pJET1.2 vector. The CloneJET® PCR cloning kit (Thermo Fischer) was used as instructed by the manufacturer to blunt and then to also ligate the *MIP1* insert into the pJET 1.2 vector. A SpeI restriction digest was performed to remove the *mip1* fragment from the pJET1.2 plasmid. This reaction contained 15 μ l pJET1.2-*mip1* DNA, 6 μ l 10xCutsmart™ buffer, 36 μ l water, and 3 μ l SpeI enzyme in a total volume of 60 μ l. pIBB103 was digested with SpeI enzyme as above. Both digested samples were column purified using the Wizard® Plus SV DNA cleanup kit (Promega) according to the manufacturers instruction and resuspended in 50 μ l water. The linearized pIBB103 was treated with Calf intestinal alkaline phosphatase (CIAP), which removed the phosphate group from the 5' ends of its DNA, in order to prevent self-ligation.

Three ligation reactions were carried out to place the *mip1* fragment within the pIBB103 RNAi vector. The ligation reactions contained 4.5µl pIBB103, with 0µl, 2µl, or 3µl purified *mip1* PCR fragment, 2µl T4 DNA ligase buffer, 1µl of T4 DNA ligase, and the reaction volume was brought up to 20µl with water. Each reaction was incubated for 45 minutes at room temperature, and 4µl of each ligation reaction was transformed into 30µl of competent *E. coli* cells. These transformations were plated on LB plates that contained 100µg/ml ampicillin, and allowed to grow overnight at 37°C.

Eight colonies from each experimental plate were grown overnight in LB +AMP broth and plasmid DNA mini preps were performed for each using the Wizard® Plus SV Minprep kit (Promega) following the manufacturer's instructions. The plasmid DNA was resuspended in 75µl water. A SpeI restriction digest was performed to confirm the correct cloning of *mip1* into the pIBB103 vector. This reaction contained 4µl pIBB103 *mip1* DNA, 1.5µl Cutsmart™ buffer, 8.5µl water and 1µl SpeI enzyme in a total reaction volume of 15µl.

F. Making the *MIP1*-mCherry NEO^R plasmid

The *MIP1*-mCherry construct was made in the pLK25 plasmid that contains a bacterial origin of replication, an ampicillin^R gene for selection within bacteria, and a NEO^R gene for selection in yeast (see Figure 2). The mCherry fluorescent protein-coding gene is present within this plasmid directly downstream of an XbaI restriction site.

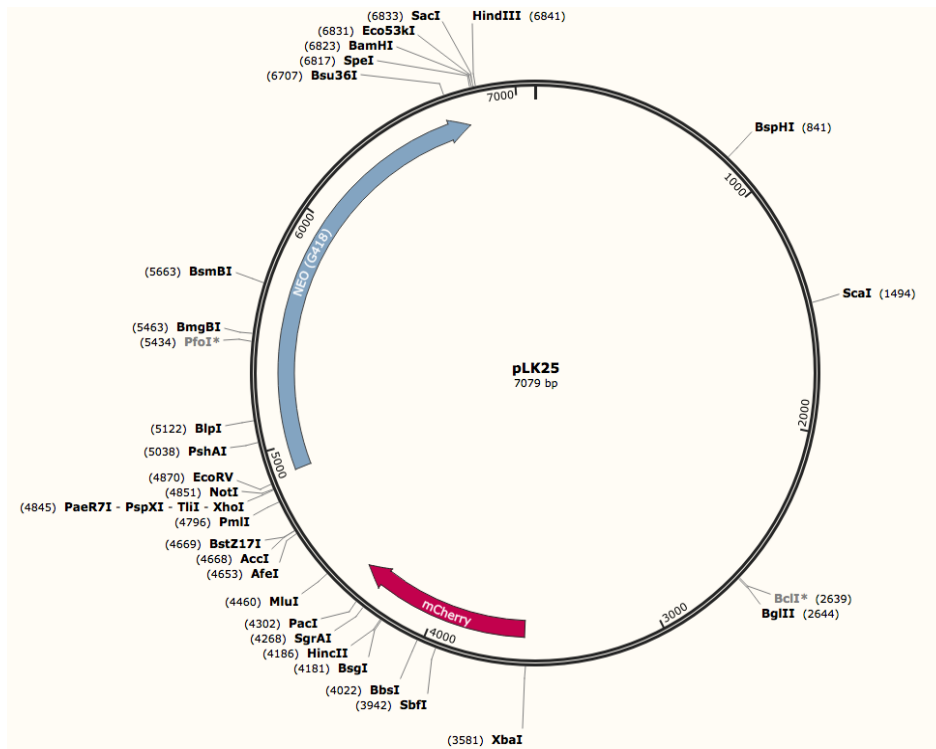


Figure 2. pLK25 vector used for *MIP1* localization.

The endogenous *MIP1* gene along with its promoter (562bp of 5' DNA) was PCR amplified from KN99 *mat α* (IBC N2) genomic DNA using the primers BLO144 and BLO 145 (see Table 1). This reaction contained 32.5 μ l dH₂O, 10 μ l Phusion HF 5x buffer, 2.5 μ l 10 μ M BLO144, 2.5 μ l 10 μ M BLO145, 1 μ l dNTP's, 0.5 μ l Phusion® Taq polymerase, and 1 μ l KN99 *mat α* genomic DNA as template. The conditions of this PCR reaction were 98°C 30s; 30 x (98°C 10s, 58°C 10s, 72°C 3:00m); 72°C 5m. The products of this PCR reaction were column purified using the Wizard® SV Gel and PCR Clean-up System (Promega) following the manufacturer instruction, and resuspended in 50 μ l of water.

The CloneJET® PCR cloning kit (Thermo Fischer) was used according to the manufacturer's instructions to blunt, and then ligate the *MIP1* insert into the pJET1.2 vector. 7 μ l of ligation mixture was transformed into 40 μ l of high efficiency competent *E. coli* cells, plated

onto LB plates containing 100µg/ml ampicillin, and allowed to grow overnight at 37°C. Seven colonies were inoculated into LB +AMP broth and grown at 37°C overnight with aeration. Plasmid mini preps were made with 1.5mls of each culture using the Wizard® Plus SV Minprep kit (Promega) and resuspended in 75µl water. DNA from each mini prep was digested using 4µl pJET1.2-*MIP1* plasmid DNA, 1.5µl Cutsmart™ buffer, 8.5µl water, and 1µl XbaI enzyme in a total reaction volume of 15µl. PCR reactions were performed on each mini prep DNA using primers WBO1 and WBO5 (see Table 1) to further confirm the presence of the *MIP1* gene in the plasmid. The reaction mix contained 12.5µl 2x Taq Mastermix (Promega), 1µl 10µM WBO1, 1µl 10µM WBO5, 0.75µl DMSO, and 9.75µl water. The conditions of the PCR reaction were 94°C 1m; 30 x (94°C 15s, 60°C 30s, 72°C 2:30m); 72°C 10m.

The *MIP1* gene along with its promoter was removed from the pJET 1.2 plasmid by XbaI restriction digest. The reaction contained 20µl *MIP1*-pJET 1.2, 6µl Cutsmart™ buffer, 31µl water, and 3µl XbaI enzyme in a total reaction volume of 60µl. The insert was gel purified using the Wizard® Plus SV DNA cleanup kit (Promega) and resuspended in 50µl water. pLK25 (see Figure 2.) was linearized using 15µl pLK25 plasmid DNA, 5µl Cutsmart™ buffer, 28µl water, and 2µl XbaI enzyme in a 50µl total reaction volume. XbaI was heat inactivated at 65°C for 20min, and 1µl CIAP was added to the reaction. The reaction was incubated at 37°C for 1 hour.

Three ligation reactions were prepared to clone *MIP1* into pLK25. These ligations contained 2µl pLK25 plasmid DNA, 2µl T4 DNA ligase buffer, 1µl T4 DNA ligase, and 0µl, 2µl, or 4µl *MIP1* insert in a final volume of 20µl with water. The ligations were incubated at room temperature for 2 hours, and 4µl of the ligation mixture was transformed into 40µl high efficiency competent *E. coli* cells. These transformants were plated onto LB plates with 100µg/ml ampicillin.

To check for the presence of *MIP1* and promoter in the pLK25 vector a PCR reaction using the forward primer WBO1 and the reverse primer WBO5 (see Table 1) was carried out as in F (i). A BglIII digest was performed on the plasmid in order to determine the orientation in which the gene was cloned into the plasmid. This digest was carried out using 4µl pLK25-*MIP1* plasmid DNA, 1.5µl 10XCutsmart™ buffer, 1µl BglIII enzyme, in a final volume of 15µl with water.

G. Making the *CTR4p-MIP1-mCherry (NEO^R)* Plasmid

The *CTR4* promoter from the p*CTR4-2* plasmid (pIBB236) was amplified by PCR using primers BLO171 and BLO172 (see Table 1). The PCR reaction contained 1µl p*CTR4-2p* plasmid template, 5µl Q5 reaction buffer, 0.5µl dNTP's, 1.5µl 10µM BLO171, 1.5µl 10µM BLO 172, 0.75µl DMSO, 0.3µl Q5® High-Fidelity polymerase (NEB), and 14.5µl water. The thermocycling conditions were as follows: 98°C 30s; 30 x (98°C 10s, 67°C 30s, 72°C 60s); 72°C 2m.

25µl pLK25 plasmid DNA was digested using 2µl XbaI in 60µl final volume, column purified using the Wizard® Plus SV DNA cleanup kit (Promega), and resuspended in 50µl water. The purified *CTR4* promoter fragment was cloned into the XbaI site of pLK25 vector using NEBuilder® Hifi DNA Assembly (NEB). The Hifi ligation reaction contained 1:3 vector: insert (2.1µl pLK25, 0.3µl *CTR4p*) DNA, 10µl Hifi MM, and 7.6µl water. A negative control reaction was performed and contained 2.1µl pLK25, 0µl *CTR4p*, 10µl Hifi MM, and 7.9µl water. The ligations were incubated at 50°C for 15 minutes. 2µl Hifi reactions were transformed into 50µl high efficiency competent *E. coli*. The transformants were plated on LB plates with 100µg/ml ampicillin. Since the AvrII site is contained within the forward primer and is part of the PCR fragment, plasmid DNA from 10 transformants were digested with AvrII to confirm

the presence of the insert. The reaction mixture contained 4µl miniprep DNA, 1.5µl Cutsmart™ buffer, 9µl water and 0.5µl AvrII in a total reaction volume of 15µl.

After *CTR4p* had been cloned into pLK25, the *MIP1* gene was cloned downstream of the promoter. A PCR amplification reaction was used to amplify *MIP1* from KN99 *matα* genomic DNA using the primers BLO179 and BLO180 which contain overlaps to the *CTR4p*-pLK25 vector sequence for Hifi cloning. The reaction mix for this PCR contained 10µl Q5 reaction buffer, 3µl 10µM BLO179, 3µl 10µM BLO180, 1.5µl DMSO, 1µl dNTP's, 2µl Q5® High-Fidelity polymerase, 29µl water, and 1µl KN99 *matα* genomic DNA as the template. The conditions for thermocycling were 98°C 30s; 30 x (98°C 10s, 58°C 30s, 72°C 2:30m); 72°C 2m. An AvrII digest was carried out in order to linearize the pLK25-*CTR4p* plasmid, and prepare it for *MIP1* cloning. Both the *MIP1* amplicon, as well as the AvrII digested pLK25-*CTR4p* were column purified using the Wizard® Plus SV Miniprep kit (Promega) and resuspended in 50µl water.

NEBuilder® Hifi DNA Assembly (NEB) technology was used to insert place the *MIP1* gene in the pLK25-*CTR4p* plasmid, in frame with the mCherry tag. The Hifi ligations contained 1:3 molar ratio of vector: insert DNA with 1.5µl *CTR4*-pLK25, 1.13µl or no *MIP1* PCR fragment, 10µl Hifi master mix, in a total reaction volume of 20µl with water. Both ligation reactions were incubated at 50°C for 15 minutes. Transformations were carried out by placing 2µl of Hifi ligation mixes into 45µl of competent *E. coli* cells. Transformations were plated onto LB plates with 100µg/ml ampicillin, and grown overnight at 37°C. Plasmids from eight colonies were used to PCR amplify the *MIP1* gene. The reaction mix contained 5µl Q5 reaction buffer, 0.5µl dNTP's, 1.5µl 10µM BLO179, 1.5µl 10µM BLO180, 0.75µl DMSO, 0.3µl Q5® High-

Fidelity polymerase, 1µl plasmid prep DNA, and 14.5µl Water. The reaction conditions were identical to the previous *MIP1* amplification using these primers.

H. Making the pGDPp-*MIP1*-GFP Plasmid

The *MIP1* ORF gene containing overlaps for Hifi cloning into the pGDPp-GFP vector was PCR amplified. The reaction mix for this PCR contained 5µl Q5 reaction buffer, 0.75µl of dNTP's, 1.5µl 10µM BLO 191, 1.5µl 10µM BLO 192, 0.5µl Q5® High-Fidelity polymerase, 13.65µl water, and 1µl KN99 *matα* genomic DNA as template. The reaction conditions used were 98°C 30s; 30 x (98°C 10s, 62°C 30s, 72°C 2:30m); 72°C 2m. The pGDPp-GFP vector was linearized using the restriction enzyme EcoRI in a reaction mix containing 10µl GPD-GFP vector, 4µl 10XFastDigest™ buffer, 24µl water, and 2µl EcoRI enzyme in a total volume of 40µl. This reaction was incubated at 37 °C for 6 hours. The digested pGDPp-GFP and the amplified *MIP1* were column purified using the Wizard® Plus SV DNA cleanup kit (Promega) and resuspended in 50µl water.

The *MIP1* fragment was ligated into the linearized pGDPp-GFP plasmid as follows. Two ligation reactions were performed in order to place *MIP1* into the plasmid. The reactions contained 5µl pGDPp-GFP vector, 1.1µl, or no *MIP1*, 10µl Hifi master mix, and each reaction was brought up to a total volume of 20µl with water. Both reactions were incubated at 50 °C for 15 minutes. Transformations of the Hifi ligations were carried out by placing 2µl of each ligation into 50µl of competent *E. coli*. Transformations were grown on LB plates containing 100µg/ml ampicillin overnight at 37°C. Eight colonies were selected from the experimental plate and inoculated into LB+AMP broth. Minipreps were performed on the eight cultures using the Wizard® Plus SV Minprep kit (Promega) and resuspended in 75µl water. *MIP1* was confirmed by using PCR amplification using BLO191 and BLO192 as previously described.

I. Transforming *C. neoformans* by Electroporation

Electroporation mediated transformation of *C. neoformans* was carried out as follows. Strains to be transformed were cultured in approximately 25ml of appropriate media and allowed to grow overnight at 30°C with shaking at 180rpm. After 16-18h of growth, this culture was diluted to approximately 5×10^6 cells/ml with the appropriate media and allowed to grow for an additional 4 hours. The culture was centrifuged at 4,000rpm in an Eppendorf MiniSpin™ centrifuge, and washed twice with 50ml sterile DI water in order to remove any excess media, and once with electroporation buffer (10mM Tris-HCl, pH7.5, 1mM MgCl₂, 270mM sucrose). The samples were then treated with 200µl of 1M DTT in 50ml of electroporation buffer, and incubated for 10 minutes on ice. The culture was washed with electroporation buffer as above. The supernatant was discarded and the pelleted cells were resuspended in the residual buffer. Then 60µl of this mix was placed into a 0.2cm electroporation cuvette. The appropriate DNA was added to this culture and electroporation is carried out with the settings of 0.5kV, 25µF, and either 1000 or ∞ ohms. Pulse length or time constants of 15-25msec gave the best results. Samples were resuspended in YPD broth for 2 hours before plating on appropriate selection media.

i. Electroporation of JEC21 cells with the pIBB103-*MIP1* (MIP1i) construct

pIBB103-*MIP1* was linearized with I-SceI. This reaction contained 25µl pIBB103-*MIP1*, 6µl 10XCutsmart™ buffer, 27.5µl water and 1.5µl I-SceI enzyme in a total reaction volume of 60µl. This linearized DNA was purified using the Wizard® Plus SV DNA cleanup kit (Promega), and resuspended in 50µl water. Electroporation was carried out using 6µl pIBB103-*MIP1* and 60µl of JEC21(Serotype D) cells. A negative control was performed by electroporation of 60µl JEC21 cells with no DNA. The time constants for the +DNA reactions

ranged from 31ms to 142ms. The time constants for the –DNA reactions were 28ms to 81ms. These reactions were both plated onto YPD-NEO plates and allowed to grow for 4 days at 30°C.

ii. Electroporation of KN99 *mat α* cells with the *pLK25-MIP1* or *pLK25-CTR4p-MIP1* constructs

Linearization of *pLK25-MIP1* or *pLK25-CTR4p-MIP1* was performed using the restriction enzyme NotI. The reaction contained 20ul plasmid DNA, 6ul 10xNEB 3.1™ buffer, 32ul water, and 2ul NotI enzyme in a total reaction volume of 60ul. This linearized DNA was column purified and resuspended in 50ul water. Electroporation was carried out using 4ul *pLK25-MIP1* or 6ul *pLK25-CTR4p-MIP1* in 60ul of KN99 α cells. Negative controls were performed by electroporation of 60ul KN99 α cells with no DNA. The time constants for the +DNA reactions ranged from 47ms to 118ms and 71ms to 128ms, respectively. The time constants for the –DNA reactions ranged from 21ms to 89ms and 43ms to 71ms, respectively. These reactions were both plated onto YPD-NEO plates and allowed to grow for 4 days at 30°C.

YPD/Neo broth containing 200 μ M bathocuproine disulfonic acid (BCS) (Sigma-Aldrich) and CuSO₄ at concentrations of 25 μ M and 50 μ M were made to test *CTR4p-MIP1* transformants.

J. Biolistic Transformation

In order to stably integrate a DNA construct into the genomic DNA of *C. neoformans* biolistic incorporation was utilized. Biolistic incorporation was carried out using the method described by Bose et al.⁷⁶ All biolistic transformations were carried out on YPD plates containing 1M sorbitol before transferring the cells to the appropriate selective medium.

Briefly, the method described requires the binding of the desired DNA construct onto golden beads. These beads are then placed onto a disc and compressed helium is used to launch the DNA bound beads into the *C. neoformans* culture that is evenly spread across a YPD-1M-

Sorbitol plate. Once biolistics is carried out the cells are allowed to grow for 4-6 hours and then scraped from the YPD plate and spread onto plates containing the appropriate selective media for the selection of transformed colonies.

K. Growth Curves

Colonies were allowed to grow overnight at 30°C in appropriate liquid media. Each culture was divided in two and centrifuged for 3m at 14,500rpm. One half of each culture was washed three times with sterile PBS and re-suspended in 30ml of YPG-NEO, the other half of each culture was re-suspended in 30ml of YPD-NEO. After 3h each sample that contained YPG-NEO was spun down and resuspended into YPG-NEO broth that contained 5-FOA (concentrations given with each experiment). At the time points 0h, 3h, 6h, 9h, 12h, and 24h 2ml of each sample was collected, and fixed in 3.5% formaldehyde. Absorbance at 600nm was used to determine culture density for each sample.

i. Determination of effective 5-FOA levels in growth curves

To determine an appropriate level of 5-FOA that will select for robust RNAi but not be toxic to all cells in liquid culture, a growth curve was performed using various levels of 5-FOA. This experiment was carried out using the protocol for growth curves described previously (see Methods K), adding 5-FOA levels that were 0.0, 0.125, 0.250, and 0.5mg/ml at the 3h point. Samples were taken at 6h and 24h for growth analysis.

L. Mitotracker™ Green Live Cell Assay

The following assay was designed to determine the mitochondrial integrity of cells under varying growth conditions. Cells that were grown under varying conditions were incubated in 500µl sterile PBS containing 0.2µM Mitotracker green live cell dye, covered with foil, and incubated with shaking at 30 °C. The cells were then centrifuged at 13,400 rpm for 5 minutes,

washed 3 times with 500 μ l of sterile PBS, and resuspended in 200 μ l sterile PBS. 10 μ l of each sample was placed on a clean glass slide for imaging, two images were taken for each sample.

For this work each image was taken using the EVOSTM FL Auto microscope in the biology department at WCU, using the GFP light cube (395 wavelength). Each image was saved using the settings of 79 light intensity, and 73 exposure, and 0 gain. All images were taken using the 40X objective. Quantification of light intensity within pictures was carried out by taking an 81nm area of centralized regions within 15 separate cells selected at random and using the measure function within imageJ to obtain an average fluorescent light intensity within the area selected. The value produced from each of the 15 cells measured were averaged together, producing a single value that represented the fluorescent intensity of all cells within the image. Average background was subtracted within each image by selecting 15 random points of 81nm throughout the image that did not contain a cell, and using the measure function to determine the intensity of fluorescence within these points. The intensity of each of these 15 points were averaged together, and subtracted from the overall average value of light intensity collected from cells within the same image. This value represented the average fluorescent intensity of cells within an image that had been adjusted for background fluorescence.

M. Deconvolution of MitotrackerTM Stained Images

Image deconvolution was performed in FIJI using the Iterative Deconvolve 3D plugin.⁸⁰ This plugin is partially based on the DAMAS algorithm by Thomas F. Brooks and William M. Humphreys, Jr., NASA-Langley Research Center. The settings used included an anti-ringing step, low pass filter (x,y,z) set to 1.0, and 10-15 iterations.

N. Primers Used

Table 1. Primers used in this project

Name	Description	Sequence (5' to 3')	Amplicon Length (bp)	Restriction Enzyme
BLO144	CnMIP1 F	cccaaatctagaCAATATGAGTGTGTAGCCAG	5075	XbaI
BLO145	CnMIP1 R	cccaaatctagaTTGAAACTTCTTGCTAGAA	5075	XbaI
BLO179	CnMIP1 F	gacaacgacttcaccaatccATGCGCAAGGCGCTTGATATTTTC	4513	NA
BLO180	CnMIP1 R	ctcgcccttgctcaccattcTTGAAACTTCTTGCTAGAAGACAGAAC	4513	NA
BLO191	CnMIP1F	atactgcataaatacaatgaattctATGCGCAAGGCGCTTGATATTTTC	4513	NA
BLO192	CnMIP1 R	gctcctcacccttggaatgaattctTTGAAACTTCTTGCTAGAAGACAGAAC	4513	NA
BLO163	MIP1 SpeI F	TTTACTAGTcaagctctcttgatctc	259	SpeI
BLO164	MIP1 SpeI R	TTTACTAGTcatctgaatagtactggctc	259	SpeI
WBO1	Exon 1 F (MIP1)	ATGCGCAAGGCGCTTGATATTTTC	281	NA
WBO5	Exon 1 R (MIP1)	GGATTTGCGAATCTTCCTAACTCGAGGCTGGCCATAGC	281	NA

CHAPTER III. RESULTS

A. Identifying *C. neoformans* *MIPI* Gene by Sequence Homology

DNA polymerase gamma (DNA polG) has been studied extensively in *S. cerevisiae*, and humans, but not in *C. neoformans*. Since *C. neoformans* is an aerobic organism, we hypothesized that DNA polG will be essential to mitochondrial function, and ultimately the survival of the organism. Therefore, to better understand this function in *C. neoformans*, the presence of this gene(s) in the cryptococcal genome was determined. A BLAST search of the H99 Serotype A, as well as JEC21 Serotype D genome against the *S. cerevisiae* DNA polG protein sequence identified one gene (CNAG_06769) in *C. neoformans* with a high probability of encoding this enzyme (Figure 3). The gene showed a 45% identity, and a 58% similarity between the amino acid sequences within Serotype A (Figure S1). Only one *MIPI* homolog was found in *C. neoformans*. In order to determine if Primase polymerase was present within *C. neoformans* a BLAST search of the same *C. neoformans* genomes against the human PrimPol protein sequence identified no homologs within *C. neoformans*.

Job title: Protein Sequence (1254 letters)

RID 06VFED53014 (Expires on 11-10 03:49 am)

Query ID lcl|Query_201962

Description None

Molecule type amino acid

Query Length 1254

Database Name nr

Description All non-redundant GenBank CDS translations+PDB+SwissProt+PIR+PRF excluded environmental samples from WGS projects

Program BLASTP 2.7.1+ [► Citation](#)

Other reports: [► Search Summary](#) [\[Taxonomy reports\]](#) [\[Distance tree of results\]](#) [\[Multiple alignment\]](#) [\[MSA viewer\]](#)

New Analyze your query with [SmartBLAST](#)

+ [Graphic Summary](#)

▾ [Descriptions](#)

Sequences producing significant alignments:

Select: [All](#) [None](#) Selected:0

[↑↓](#) [Alignments](#) [Download](#) [GenPept](#) [Graphics](#) [Distance tree of results](#) [Multiple alignment](#) [⚙](#)

	Description	Max score	Total score	Query cover	E value	Ident	Accession
<input type="checkbox"/>	DNA polymerase gamma 1 [Cryptococcus neoformans var. grubii H99]	498	791	75%	8e-154	45%	XP_012047111.1

Figure 3. Amino acid BLAST search comparing the *C. neoformans* genome against the *S. cerevisiae* DNA polG sequence.

Several conserved protein domains are present in the putative *C. neoformans* DNA polymerase gamma protein shown in Figure 4, that are also present within the *S. cerevisiae* protein. Alignment between the polymerase domain of *S. cerevisiae*, and *C. neoformans* shows a 62% identity and 76% similarity between the species. Both proteins also contain contain a MLS. The high sequence similarity to *S. cerevisiae* DNA polG (ScpolG), as well as the presence of a conserved polymerase domain suggests that CNAG_06769 gene in *C. neoformans* encodes the DNA polymerase gamma protein. However, there are certain domains that differ between the DNA polG proteins in the two species. Two domains of unknown function are present within the *C. neoformans* protein, while *S. cerevisiae* has a much longer C terminal extension (Figure 5).

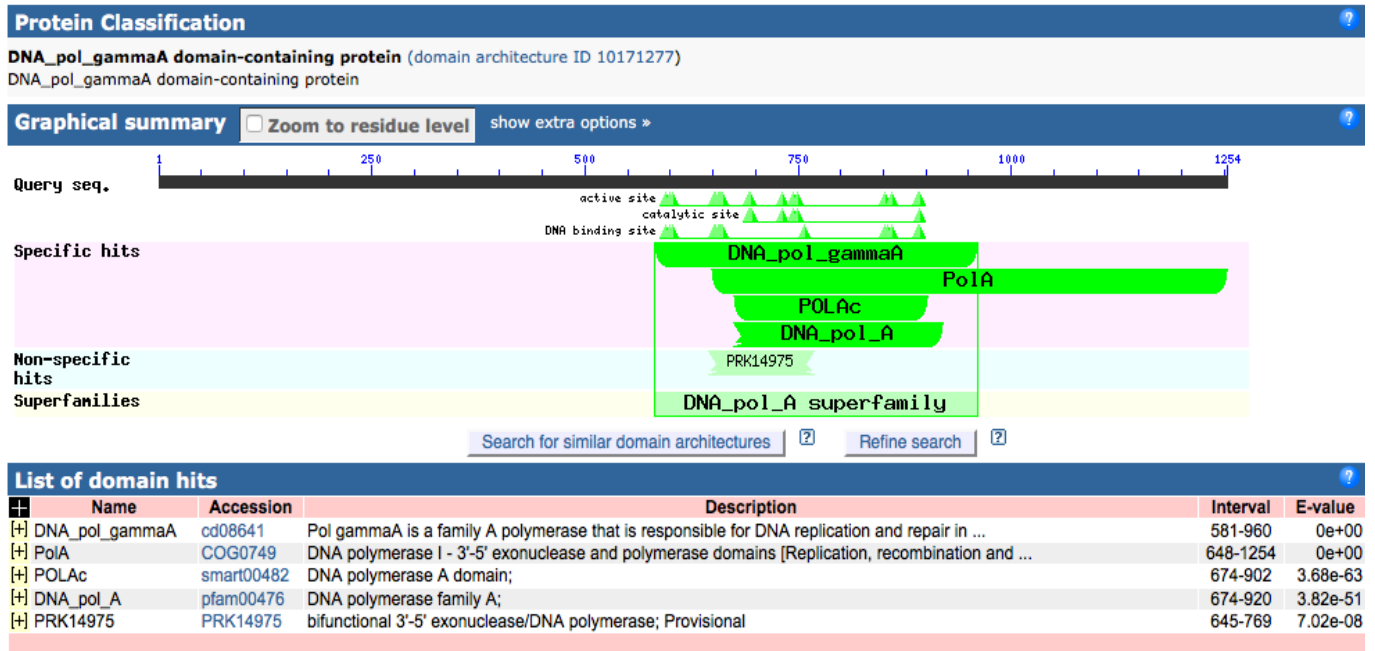


Figure 4. Presence of conserved domains within the DNA polymerase gamma homolog found within *C. neoformans*.

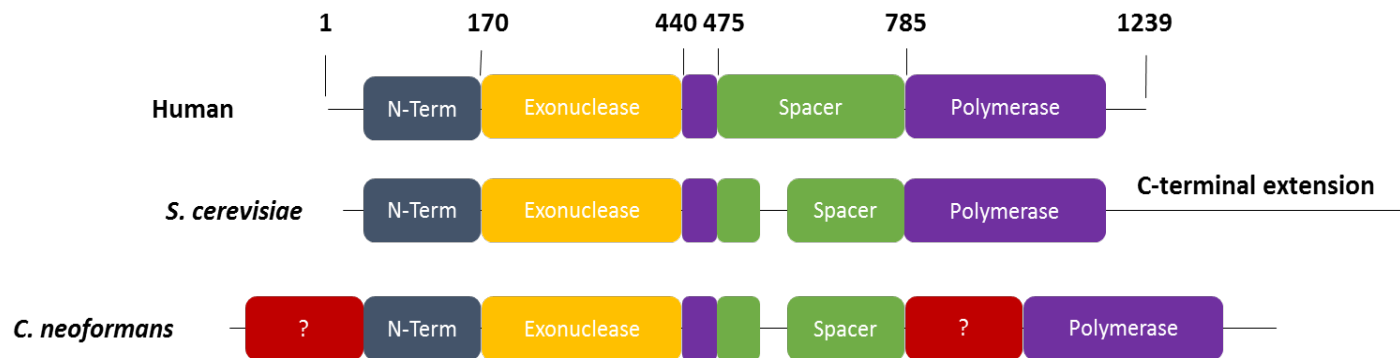


Figure 5. Domain alignment of DNA polG amino acid sequences from human (top), *S. cerevisiae* (middle), and *C. neoformans* (bottom). This alignment was created using domain predictions from the National Center of Biotechnology Information's online BLAST database.

The two domains of unknown function that have been identified within *C. neoformans* appear to be unique to this organism. BLAST searches reveal no homologous domains within DNA polG of other known organisms. Function of these regions of the protein is unknown.

B. Determining the Essentiality of DNA Polymerase Gamma in *C. neoformans* by RNA Interference

Since *C. neoformans* is an obligate aerobic organism, we hypothesized that this yeast will require active mitochondria in order to survive and be virulent. The presence of a functional DNA polymerase gamma is known to be essential for the mitochondria within a cell to function properly. In order to test if DNA polG is required for survival in *C. neoformans* the CnMip1 mRNA and protein levels were knocked down *in vivo* using RNA interference.

RNAi is a process that leads to degradation of mRNA that corresponds to the sequence of double stranded RNA found within the cell. In order to check the essentiality of *CnMIP1* in *C. neoformans*, bases 697-956 of the *CnMIP1* gene was cloned into the RNAi vector, pIBB103 (Figure 1). The RNAi cassette in pIBB103 contains two galactose inducible promoters that transcribe from opposing ends of a DNA fragment and are flanked by terminators. This allows for the transcription of sense and antisense RNA to occur, functionally creating dsRNA within the cell. Within these opposing promoters and terminators is a portion of the *ura5* gene, which assists in selection on 5-FOA containing media. A *SpeI* restriction endonuclease site in between the *GAL7* promoters allows for cloning of selected sequence into the RNAi construct, in order for the associated gene to be knocked down *in vivo*. There are also telomeric regions found within the plasmid that assist with stability of the vector within yeast hosts.

Utilizing primers BLO163, and BLO164 (see Table 1), a 562bp portion of the third exon of the *CnMIP1* gene, was PCR amplified using genomic DNA from the JEC21 (Serotype D) strain as the template. An attempt to use SLIC cloning to clone the PCR amplified exonic *mip1* fragment was unsuccessful, therefore T4 DNA ligase was used. The PCR amplified exonic *mip1* fragment was cloned in the *SpeI* site of pIBB103. Figure 6(b) shows the results of the *SpeI* digest used to confirm the presence of the *mip1* fragment in four different transformants. The

restriction digest confirmed that all four selected transformants contained the correct pIBB103-*mip1* construct. The 8504bp band present at the top of figure 6 (b) correlates to the pIBB103 vector, while the 259bp band correlates to the *mip1* fragment.

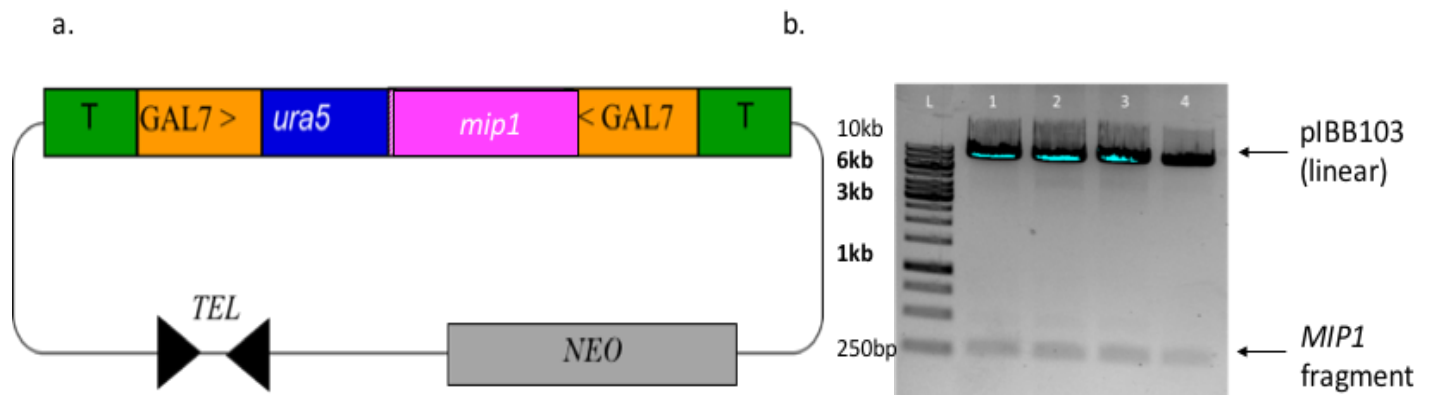


Figure 6. (a) Structure of pIBB103-*mip1* plasmid. (b) SpeI digest of pIBB103-*mip1* transformants. (1- 4 are plasmid digests from four pIBB103-*mip1* colonies; L=1kb Generuler DNA ladder).

The pIBB103-*mip1* #2 along with the empty pIBB103 vector without an insert were electroporated into the JEC21 strain. Transformants were selected by plating on YPG-NEO plates. The JEC21 strain was used for this step due to the efficiency of the *GAL7* promoter being higher than in a Serotype A strain like KN99.²⁰ Transformants streaked onto YPG-NEO (see Methods) were replica plated onto YPG-NEO containing 5-FOA in order to select for cells that are performing RNAi robustly. Figure 7 shows the results of replica plating these colonies from YPG-NEO to YPG-NEO containing 5-FOA. The colonies containing the *mip1* RNAi showed decreased growth in 5-FOA media, while the empty pIBB103 vector grew as on YPG-NEO.

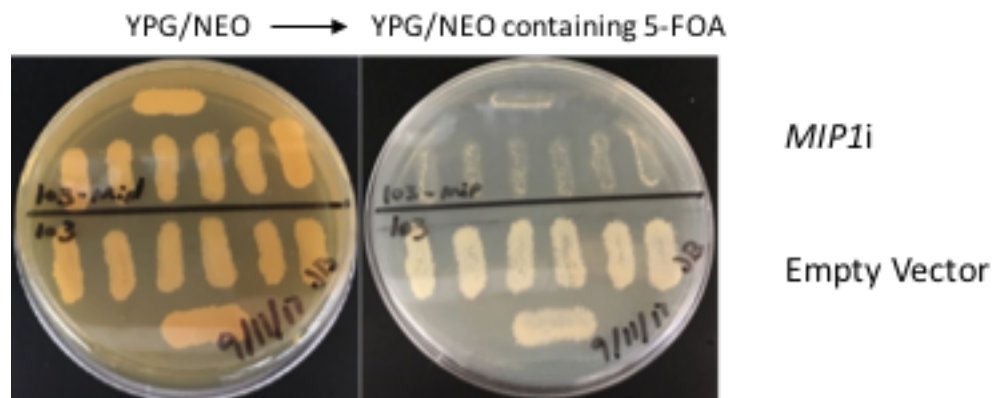


Figure 7. Replica plate of pIBB103-*mip1* (top) and pIBB103-empty (bottom) from YPG-NEO onto YPG-NEO containing 5-FOA.

C. Growth of Cells When *MIP1* Gene Product is Decreased

i. Growth of cells within YPD-NEO or YPG-NEO containing 1mg/ml 5-FOA

To determine the effect of the pIBB103-*mip1* construct on the survival and growth of transformed colonies, three colonies containing the pIBB103-*mip1* plasmid, and one colony containing the empty pIBB103 plasmid were grown overnight in YPD-NEO media. After overnight growth at 30°C these cultures were divided with one half remaining in YPD-NEO media, while the other half of the culture was centrifuged and resuspended with YPG-NEO media. At the 3hour time point the cultures containing YPG-NEO media were centrifuged and re-suspended with YPG-NEO media containing 1mg/ml 5-FOA. Aliquots of 2mls were collected at different time points, and culture densities were determined spectrophotometrically. The results were normalized and are shown in Figure 8.

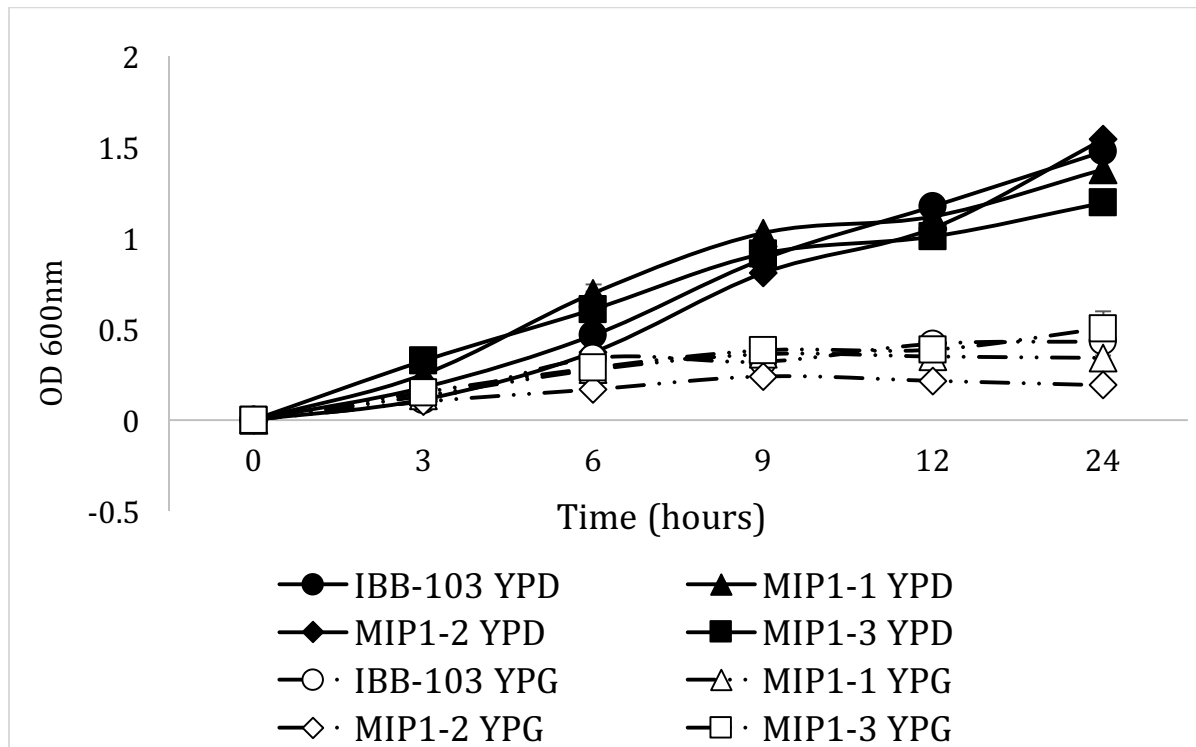


Figure 8. OD600 readings of cells containing either the pIBB103-*mip1* construct, or the pIBB103 construct. Time points (in hours) of sample collection are indicated. Broken lines indicate presence of YPG-NEO media, solid lines indicate presence of YPD-NEO media. 1mg/ml 5-FOA was added to all YPG-NEO cultures at the 3h time point. [Standard deviation used for error bars].

Although all cultures grew well in YPD-NEO as expected, they all grew poorly in YPG-NEO media containing 1mg/ml 5-FOA. This was initially puzzling, since pIBB103 cells appear to grow on YPG-NEO plates with 1mg/ml 5-FOA (Figure 7). However, I hypothesized that this result was likely because the level of 5-FOA was toxic for cells to survive in liquid culture, even when robust RNAi of the *ura5* fragment was occurring.

ii. Growth of cells within YPD-NEO or YPG-NEO containing 0.2mg/ml 5-FOA

Since the previous experiment showed that the media likely contained levels of 5-FOA that were too high for cell growth, the above growth curve was repeated using two colonies containing pIBB103, and 3 colonies containing pIBB103-*mip1*, and 0.0, 0.125, 0.25, and 0.5mg/ml 5-FOA. Samples were taken for growth analysis at the 6h and 24h time points. The 0.125mg/ml 5-FOA was not able to inhibit growth well, while 5-FOA concentrations of 0.5mg/ml 5-FOA and above appeared to be toxic to all cells in liquid culture (Figure 9). However, the 0.25mg/ml 5-FOA appeared to be better tolerated by the cells with the pIBB103 plasmid. Therefore, the growth curve was repeated using two colonies that contained the pIBB103-*mip1* vector, and two colonies that contained the pIBB103 empty vector with 0.2mg/ml 5-FOA being added at the 3h time point (Figure 10).

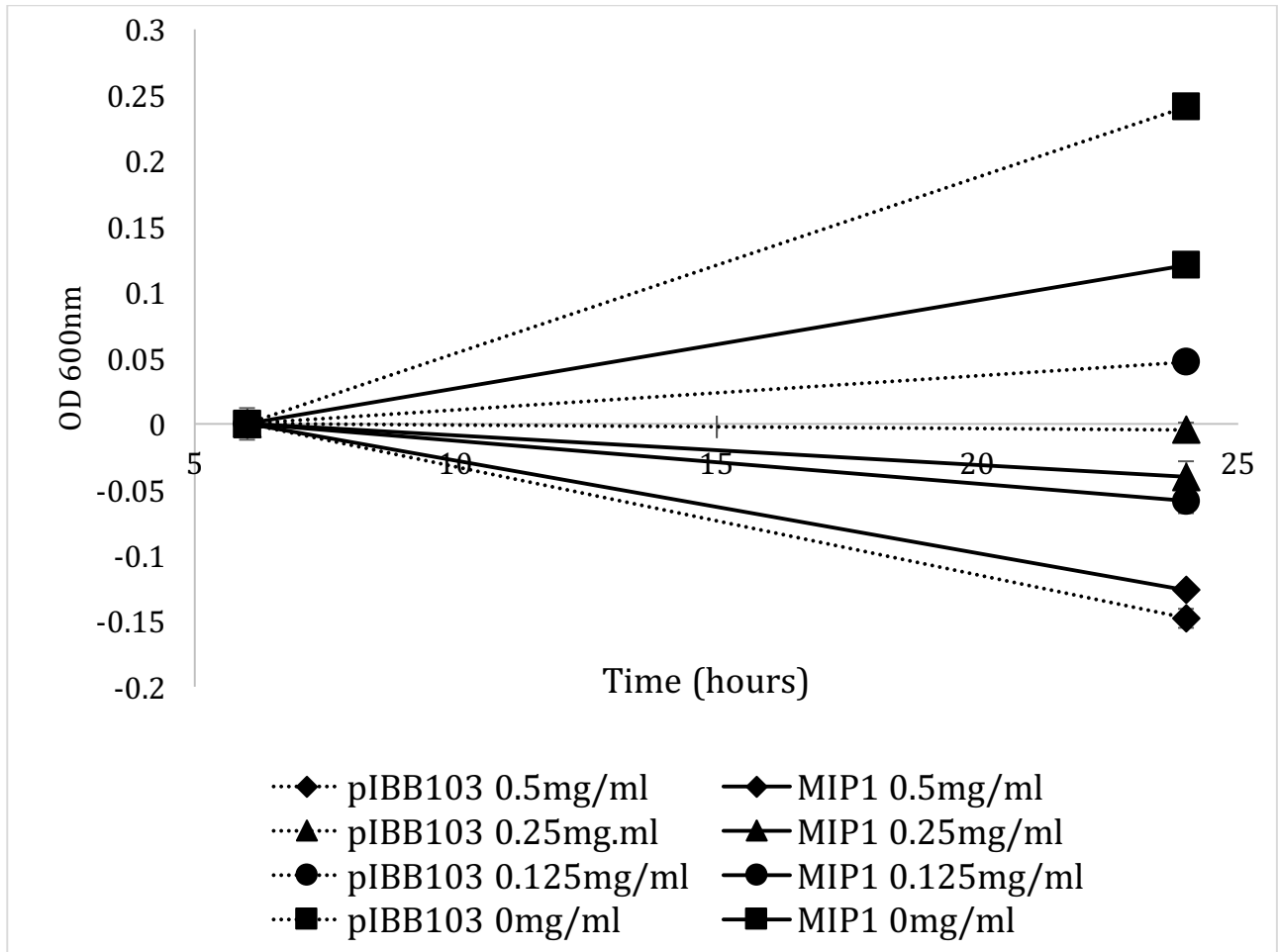


Figure 9. OD600 readings of cells containing either the pIBB103-*mip1* construct, or the pIBB103 construct. Cells containing either construct were grown for 24 hours in levels of 5-FOA that varied from 0, 0.125, 0.25, or 0.5mg/ml 5-FOA, as indicated in the figure legend. 5-FOA was added at the 3h time point for in all cultures. [Standard deviation used for error bars].

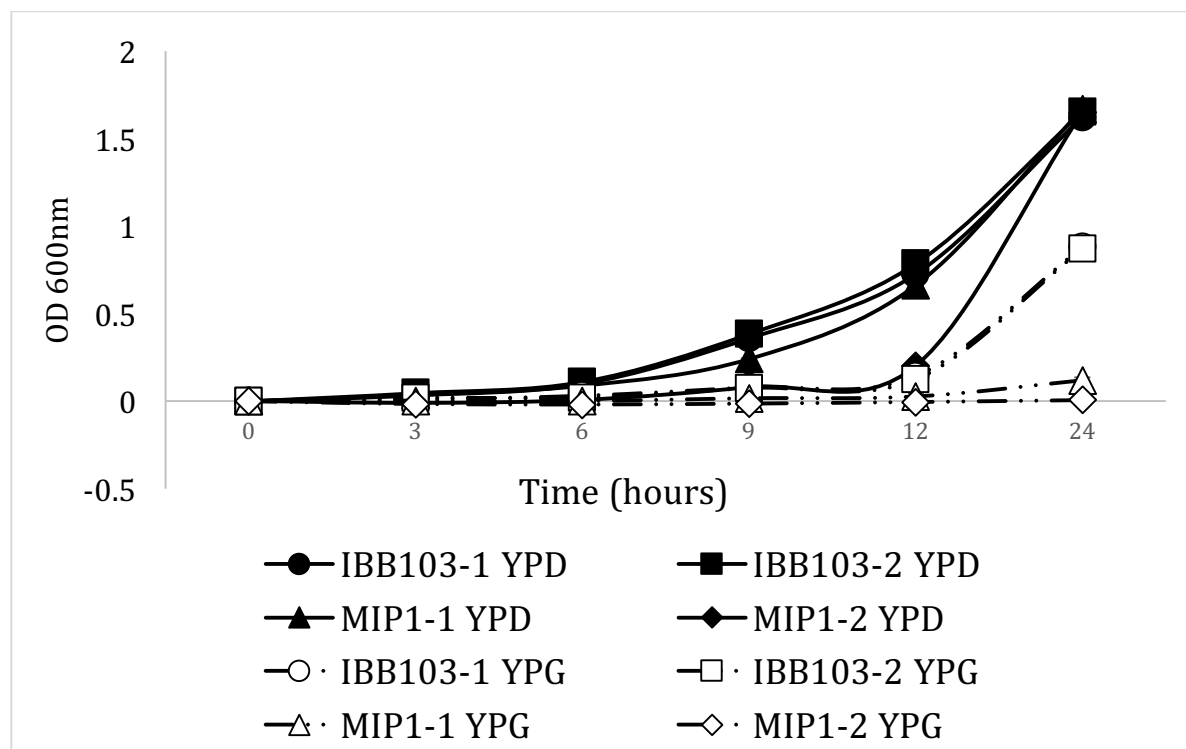


Figure 10. OD600 readings of cells containing either the pIBB103-*mip1* construct, or the pIBB103 construct. Time points (in hours) of sample collection are indicated. Broken lines indicate presence of YPG-NEO media, solid lines indicate presence of YPD-NEO media. 0.2mg/ml 5-FOA was added to all YPG-NEO cultures at the 3h time point. [Standard deviation used for error bars].

The data shown in Figure 10 indicates that colonies containing pIBB103 are able to grow in YPG-NEO media containing 0.2mg/ml 5-FOA, but those with pIBB103-*MIP1* that are actively silencing *MIP1* are unable to do so over 24 hours in the same media. All colonies grew well within YPD-NEO media.

D. Effect of MIP1p Depletion on Mitochondrial Stability

Although the RNAi studies demonstrated that the *CnMIP1* gene is essential for growth, it did not give any indication of the gene's function. The *MIP1* gene is known to affect mitochondrial function in other organisms. Therefore, to determine the effects of a reduction of

Mip1p on the state of the cells' mitochondria, cells with reduced *MIP1* mRNA (*MIP1i*) were stained with the Mitotracker Green live cell dye. This dye stains active mitochondria and is used to give an indication of mitochondrial function within each cell. We hypothesized that because *MIP1* mRNA was decreased in the presence of the pIBB103-*mip1* RNAi construct, mitochondrial stability would be lower than wild type, causing a loss of cell viability. As a result, mitochondria would no longer be able to take up the Mitotracker dye, as it would in a live cell.

i. Development of the Mitochondrial Stability Assay

In order to determine the mitochondrial stability in cells grown under varied conditions, an assay was developed that could show differences within mitochondria of the cells being studied. The mitochondria of wild type cells fluoresce brightly and fairly ubiquitously when treated with 0.2 μ M Mitotracker green dye for 30 minutes as shown in Figure 11. Cells transformed with pIBB103 were used as a positive control to identify if mitochondrial integrity was intact after incubation of cells in YPG-NEO media containing 1mg/ml 5-FOA, cells were transformed and grown as mentioned previously (see Methods L) and were incubated in sterile PBS containing 0.2 μ M Mitotracker green live cell dye. Different number of PBS washes were tried in order to obtain best results. Similarly, different light settings were tried till the best results were obtained with the settings mentioned in the Methods.

The number of brightly fluorescent cells in different cultures was not the best representation of the data since there were many cells with lower fluorescence in a culture. In order to get the best representation, I decided to quantify the average fluorescence of 15 cells found within each image. Once stained cells were imaged and processed as described within the methods it was determined that this assay was capable of showing differences in fluorescent intensity between colonies that did or did not contain polG.

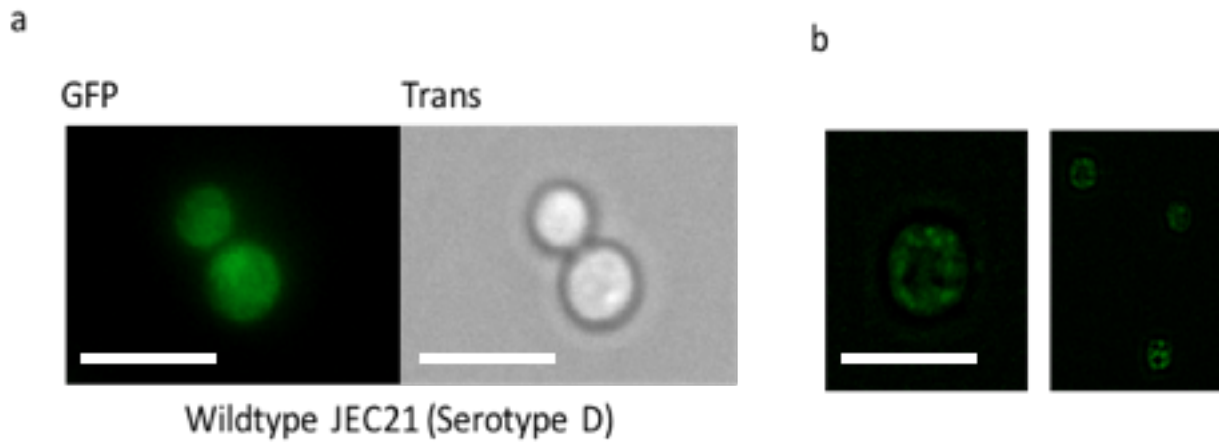


Figure 11. (a) Wild type JEC21 cell stained with $0.2\mu\text{M}$ MitotrackerTM Green live cell dye for 30 minutes. (b) Wild type JEC21 cells stained with $0.2\mu\text{M}$ MitotrackerTM Green for 30 minutes. Scale bar is equal to $20\mu\text{m}$.

ii. Mitochondrial stability is decreased in cells grown on YPGal-NEO plates

Three colonies containing the pIBB103-*mip1* plasmid, and one colony containing the empty pIBB103 plasmid were grown overnight in YPG-NEO media. These colonies were treated and imaged as described in the methods. These images were used to determine the levels of fluorescence emitted by the cells in each sample.

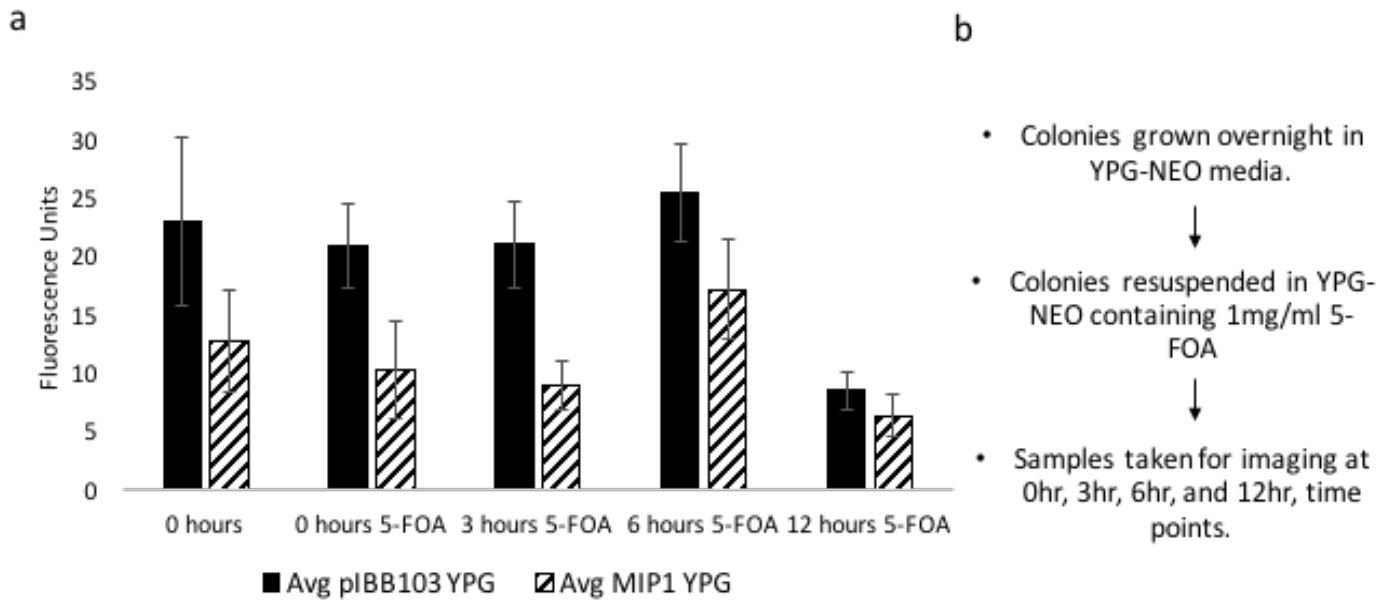


Figure 12. (a) Average levels of fluorescence emitted by cells containing either the pIBB103-*mip1* construct, or the pIBB103 construct. Presence of 5-FOA within solution is indicated above. (b) Flow chart briefly describing the experiment shown in Figure 12(a). [Standard deviation used for error bars].

The results shown in Figure 12 show that the mitochondria at time 0h had lower fluorescence intensity in the *MIP1i* colonies than the pIBB103 control. Fluorescence levels were consistently higher for pIBB103 colonies until the 12hour time point. Fluorescence levels were higher within the pIBB103 and pIBB103-*mip1* cells at the 6hours time, compared to the 3h time for an unknown reason.

iii. Growing cells from YPD-NEO that were previously not induced for RNAi

The previous experiment showed that growth of pIBB103-*mip1* cells on YPG-NEO plates after transformation was affecting the mitochondria, presumably by knocking down *MIP1* in many of the cells. Therefore, I tested whether growing the cells on YPD-NEO plates after transformation, and in YPD-NEO broth overnight would prevent this effect. Three colonies

containing the pIBB103-*mip1* plasmid, and two colonies containing the empty pIBB103 plasmid were grown overnight in YPD-NEO media and transferred to YPG-NEO media at 0h (Figure 13b). Average levels of fluorescence are shown in Figure 13a below.

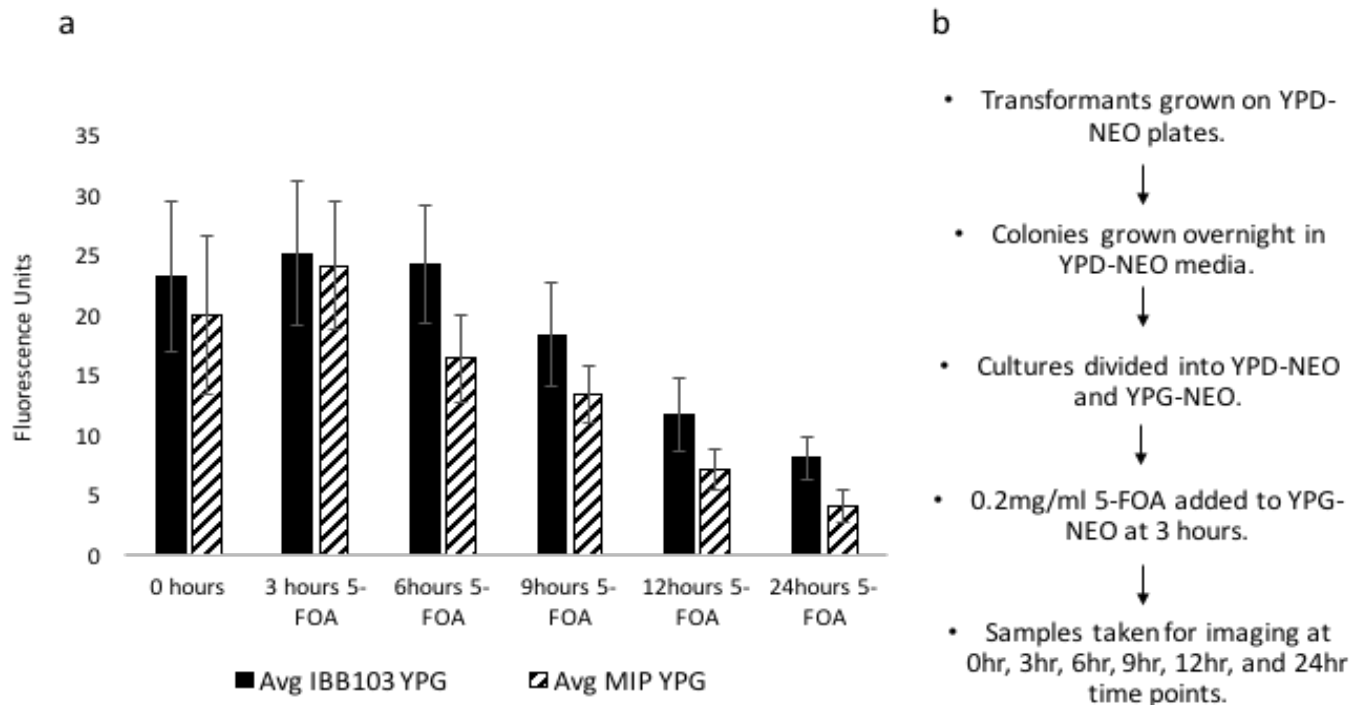


Figure 13. (a) Levels of fluorescence emitted by cells containing either the pIBB103-*mip1* construct, or the pIBB103 construct. Presence of 5-FOA within solution is indicated above. (b) Flow chart briefly describing the experiment carried out to produce the graph shown in figure 13(a). [Standard deviation used for error bars].

Growing cells in dextrose containing media prevented RNAi from occurring before the start of the experiment. As a result, fluorescence levels were higher in the pIBB103 (this should not affect cell with empty vector) containing cells throughout the 24hour incubation time, with levels of fluorescence being lower in colonies actively silencing *MIP1*. After the 6h time point all transformed cells began to show decreased fluorescence.

E. Efforts to Localize Fluorescently Tagged DNA Polymerase Gamma

In order to localize the Mip1p protein *in vivo*, a DNA construct was designed to express it from its endogenous promoter in-frame with a C-terminal mCherry fluorescent protein (Figure 2). This allows for the *MIP1* product to be followed *in vivo* using fluorescent microscopy.

The *MIP1* gene with 562bp of upstream sequence was PCR amplified from KN99 mat α genomic DNA. The product of this PCR reaction is shown in Figure 14(a). Once amplified this product was cloned into the pJET1.2 subcloning vector. Confirmation of the cloning of *MIP1* into the pJET1.2 vector, was done by restriction digestion using XbaI. As seen in Figure 14b the XbaI digest yielded two bands matching the sizes of pJET 1.2 (2974bp) as well as MIP1 (5075bp). This *MIP1* gene was removed from the pJET1.2 vector and inserted into the mCherry containing pLK25 vector (Figure 2). Six colonies from the transformation were tested for the presence of the *MIP1* gene insert by PCR amplification of the third exon of *MIP1*. Figure 15 shows that one of these colonies (#2) gave a product for the PCR and contains the *MIP1* insert.

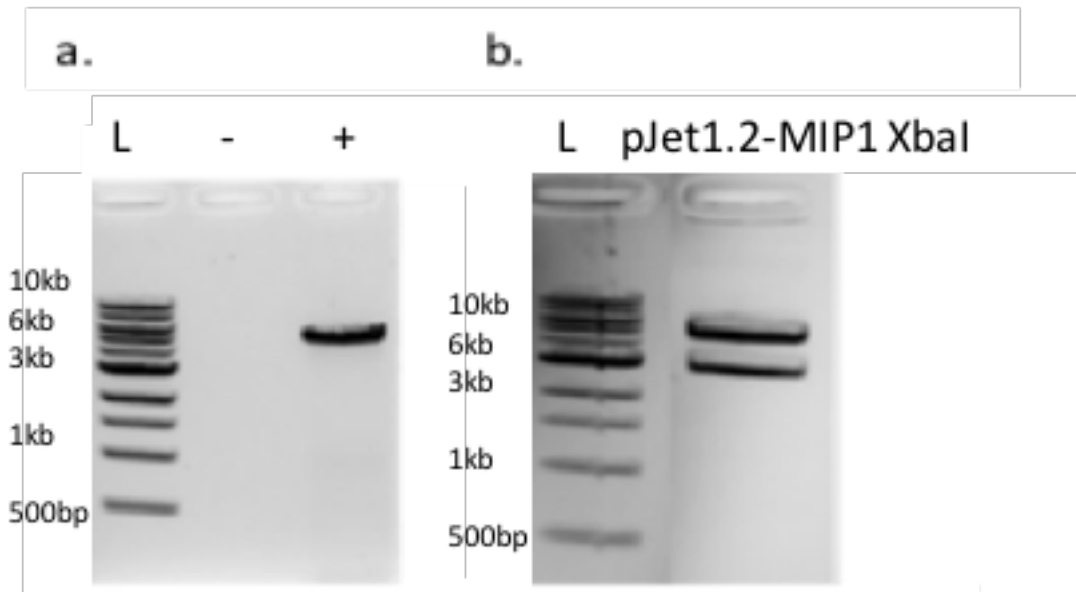


Figure 14. (a) Product of PCR reaction carried out in order to amplify the *MIP1* gene along with the genes endogenous promoter from KN99 α genomic DNA. (- indicates the negative control within the reaction. + indicates the PCR reaction containing *MIP1* along with 562bp of upstream DNA). (b) Restriction digest of plasmid DNA using *Xba*I that contains *MIP1* cloned within the pJET 1.2 cloning vector. The product of two bands that are 2793bp and 5075bp, confirms that *MIP1* was successfully cloned into the vector.

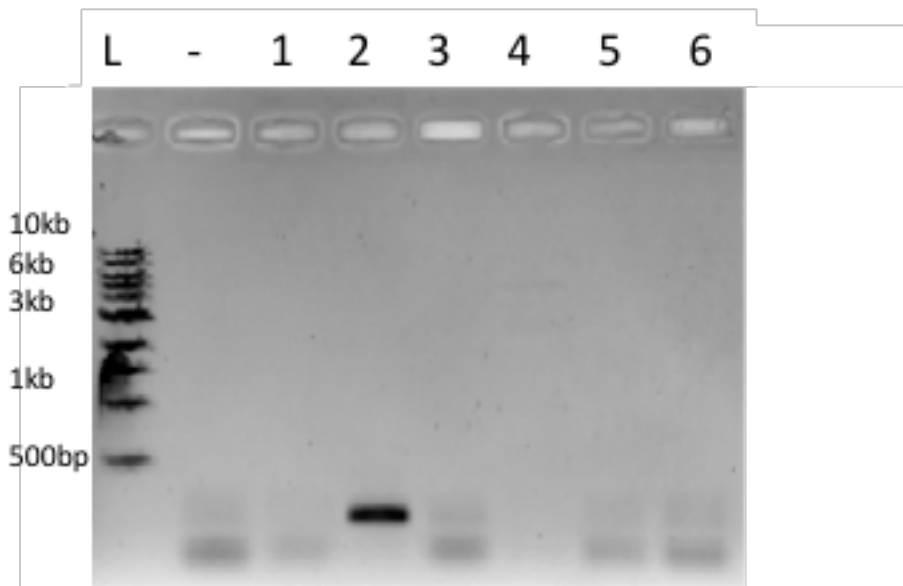


Figure 15. *MIP1* first exon PCR amplification using plasmid DNA from 6 colonies transformed by the pLK25-*MIP1* ligation reaction. The numbers 1-6 correspond to the colony from which the PCR template originated. The - corresponds to the negative control in the PCR. L contains an NEB 1kb ladder.

Electroporation, and biolistic incorporation of the pLK25-*MIP1* construct into the KN99 α strain of *C. neoformans* was carried out as described within the methods in order to determine the localization of Mip1p *in vivo*. Cells transformed via electroporation, and biolistic incorporation were prepared for viewing by growing cells in rich media overnight (YPD), and transferring cells to minimal media for 4 hours before viewing in order to reduce background fluorescence. Once prepared, cells were viewed for mCherry fluorescence, but appeared to not produce any fluorescent signal in most of the cells visualized. A minority of cells did produce signal, but numbers of cells, as well as fluorescence levels were too low to be definitive.

F. *CnMIP1* Expressed from a Regulatable Promoter

Due to the lack of consistent signal from cells containing the pLK25-*MIP1* construct described above, the *CTR4* inducible/repressible promoter was used in order to overexpress the Mip1p-mCherry protein *in vivo*. Overexpression of the fluorescent conjugate protein may allow for visualization of the protein that may be expressed at quantities too low for us to detect.

The *CTR4* promoter was PCR amplified with primers that contained overlapping sequence in the pLK25 mCherry plasmid, and inserted into the pLK25 vector linearized with XbaI upstream of the mCherry gene by NEB Hifi cloning. Ten transformants were tested in order to verify the correct ligation of the two fragments. An AvrII restriction digest was used to check the plasmids for the presence of the *CTR4* promoter, since this enzyme site was absent in the original pLK25 plasmid, but was present in the reverse primer (BLO172) that was used to amplify the *CTR4* promoter fragment. This method showed that colonies which had been linearized contained the *CTR4* promoter due to an AvrII restriction site within the primers as seen in Figure 16. Three

colonies appear to contain the *CTR4p* in pLK25 allowing for *MIP1* to be cloned behind the *CTR4p* and upstream of the mCherry fluorescent tag.

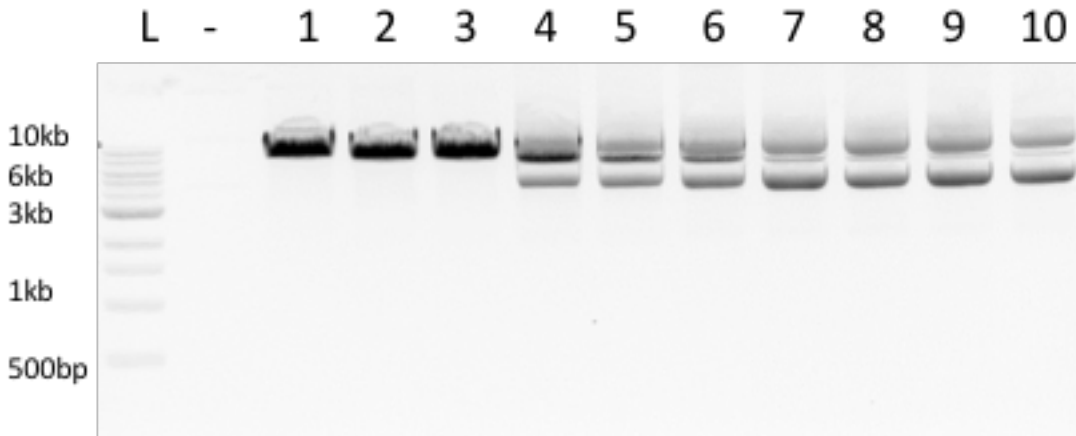


Figure 16. Results of restriction digest carried out on plasmid DNA from 10 colonies potentially transformed with the pLK25-*CTR4p* construct using the restriction enzyme *AvrII*. A single linear band in transformants 1-3 indicates that the *CTR4p* fragment is found within the vector.

The pLK25-*CTR4p* #2 construct was linearized by *AvrII*. The *MIP1* gene was PCR amplified using primers containing overlapping regions with the pLK25-*CTR4p* plasmid, and cloned into the plasmid. Four bacterial transformants were tested by PCR for the presence of *MIP1*. Three of the transformants appeared to contain an insert of the correct size (Figure 17).

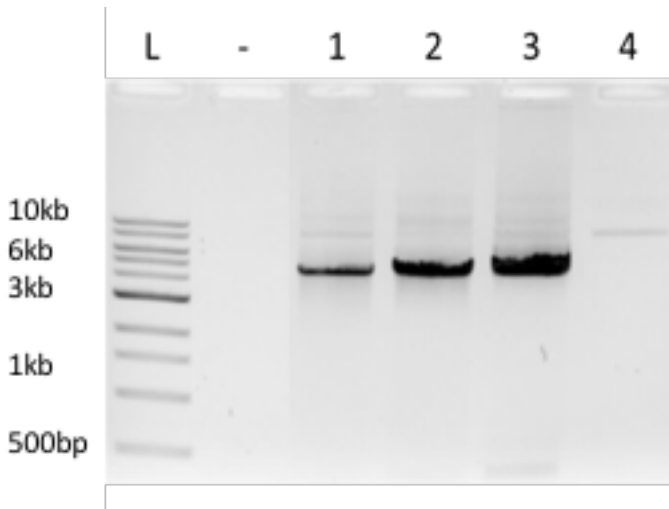


Figure 17. PCR confirmation of the presence of *MIP1* within the pLK25-*CTR4p* construct. A band present at 4513bp shows a positive result, indicating that *MIP1* is in fact present within the construct. - indicates the negative control within the reaction.

Electroporation, and biolistic incorporation of pLK25-*CTR4p-MIP1* into the KN99 α strain of *C. neoformans* was carried out to determine the localization of *MIP1* along with its mCherry tag *in vivo*, expressed from the copper repressible *CTR4* promoter. Cells containing the pLK25-*CTR4p-MIP1* plasmid were grown overnight in YPD-NEO media, and transferred to minimal media containing 200 μ m BCS for 4 h before viewing in order induce expression of the Mip1p-mCherry fusion protein of the *MIP1*-mCherry fusion protein. Unfortunately, overexpression of Mip1-mCherry did not yield good signal. As with expression from the endogenous promoter, a small minority of cells that were viewed did produce signal, but numbers of cells, as well as fluorescence levels were very low.

CHAPTER IV. Discussion

A. Identifying the *C. neoformans* *MIP1* Gene by Sequence Homology

Through amino acid alignment, the putative *C. neoformans* DNA polymerase gamma, encoded by the gene CNAG_06769, was seen to be highly conserved, with high identity to polG enzymes found in *S. cerevisiae* and humans (Figure 1 and Figure S1). Although polG is highly conserved between *C. neoformans* and *S. cerevisiae*, there are some differences that can be determined from domain alignments between the organisms. DNA polG in *S. cerevisiae* contains a C-terminal tail that is longer, by approximately 200 residues, than the C-terminal tail found in the *C. neoformans* or the human proteins.⁸¹ The *C. neoformans* polG has two regions (residues 1-135) and (residues 742-934), which are not present in any other polG protein that has been previously characterized (Figure 5). RNA seq data from multiple laboratories (Figure 18) shows that mRNA incorporating these “spacer” regions is produced under multiple growth conditions, suggesting that they are, in fact, part of the mature protein. The functions of these two spacer regions are unknown, but present an exciting opportunity for further study, and characterization. Due to the pathogenic nature of *C. neoformans*, these unknown domains could potentially be used as a drug target that can distinguish the protein found within *C. neoformans* from DNA polG found in humans, during infection.

B. Determining the Essentiality of DNA Polymerase Gamma to the Survival of *C. neoformans*

RNA interference targeted to a small portion of the third exon of *MIP1* suggests that DNA polG is essential to *C. neoformans*. Negative selection with 5-FOA was used to test for the robust action of the RNAi system in transformed cells. The *URA5* gene encodes the enzyme orotidine 5'-phosphate decarboxylase (ODCase), which catalyzes a reaction in the synthesis of the essential amino acid uracil. If cells with a functional *URA5* gene are grown on media containing 5-FOA, the action of ODCase, produces the compound 5-fluorouracil, which is toxic to the cell, and cause cell death. In the absence of *URA5* expression, such as in a Δ *ura5* strain or if RNAi efficiently silences *URA5*, ODCase is not able to utilize 5-FOA to produce 5-fluorouracil, allowing cells to survive and grow on uracil supplemented media.⁸² This has been utilized to determine the essentiality of a second gene on 5-FOA.

Negative selection on YPG-NEO plates containing 1mg/ml 5-FOA, as well as growth in liquid media containing 0.2mg/ml 5-FOA showed that colonies that contained the *MIP1i* construct did not grow on galactose containing media with 5-FOA present. Colonies that contained the empty vector were able to grow on this media. pIBB103 empty vector colonies growing in the presence of 5-FOA shows that the vector was carrying out RNAi of the *URA5* gene successfully. Cells that are only silencing *URA5* survived 5-FOA selection, but cells silencing *MIP1* as well did not survive, which indicates that the silencing of the *MIP1* gene is responsible for cell death. This result suggests that *MIP1* is essential for survival in *C. neoformans*.

Analysis of growth curves suggested that knockdown of the *MIP1* gene *in vivo* was sufficient to greatly reduce the growth of *C. neoformans* when in YPG-NEO media containing 0.2mg/ml 5-

FOA. Cells that contained the pIBB103-*mip1* construct did not grow in galactose containing media with 5-FOA present. Colonies that contained the same vector without the *mip1* fragment were able to grow on galactose containing media with 5-FOA present, although they replicated less successfully than when grown within YPD-NEO media. This decrease of growth within 5-FOA is likely due to the RNAi vector not silencing *URA5* efficiently enough to survive in some cells. RNAi is known to be a process that is not always efficient, and levels of RNA interference can greatly vary between cells.⁸³ This likely allows some cells to be capable of survival while others simply cannot carry out RNAi efficiently enough to survive.

C. neoformans is an aerobic organism that should need mitochondria to survive.⁸⁴ The knockdown of DNA polG appears to be sufficient to destroy the function of cellular mitochondria and kill these cells. The protein encoded by CNAG_06769 has been shown to have DNA polymerase activity (Wallen, personal communication). This result corresponds to previous research that has shown in other organisms, such as *S. cerevisiae*, that DNA polG is essential to the integrity of cellular mitochondria,⁵⁷ and therefore is likely essential for survival under aerobic conditions.

C. Mitochondrial Staining of Cells in the Absence of *MIP1*

Using MitoTracker Green staining, it was determined that cells containing the pIBB103-*mip1* construct, that were grown overnight in YPG-NEO broth, had a lower fluorescence signal at the start of the experiment than cells containing the pIBB103 empty construct. This result suggests that *MIP1* RNAi was likely occurring before the experiment began due to the presence of galactose in the media. Throughout the 24h incubation period colonies containing pIBB103 showed higher fluorescence than colonies containing pIBB103-*mip1*. This result led to another mitochondrial integrity experiment in which all colonies were grown in media containing only

dextrose until the experiment had begun. Dextrose prevents induction of the RNAi machinery within the cell,⁷⁶ and should stop RNAi from occurring before the experiment began.

Cells imaged after being grown overnight in YPD-NEO media showed similar fluorescence at the start of the experiment in colonies that contained pIBB103 or pIBB103-*mip1*. This indicated that the lack of galactose in the media during overnight growth, and therefore an absence of RNAi, allowed the mitochondrial stability to be uniform in all cultures at the beginning of the experiment. pIBB103 containing colonies showed higher fluorescent emission throughout the experiment than colonies containing pIBB103-*mip1*. All colonies showed lower signal after the 6hour time point. The level of fluorescence being higher within colonies that contained the pIBB103 empty vector suggests that *MIP1i* is destructive to mitochondrial stability within *C. neoformans*.

D. Localization of Mip1p

The KN99 mat α (Serotype A) strain of *C. neoformans* was transformed with the pLK25-*MIP1* plasmid in order to express the *MIP1* protein product along with an mCherry fusion protein. Once the cells containing this plasmid were treated and viewed (as described in the methods) pictures were processed using imageJ, and it was determined that no signal was present within the majority of cells transformed with this plasmid. A minority of transformed cells showed faint signal, indicating that some cells may contain the *MIP1*-mCherry fusion protein. The signal's presence not being found within all cells indicates that the protein may be expressed at levels too low to view in the majority of cells, or that the majority of cells were simply not expressing the protein. Another option to explain the lack of signal present within most cells is that the protein may be quickly degraded after being expressed, resulting in a low or absence of signal present within samples. Western blots have not yet been performed to confirm

the presence of the fusion protein in the cell. In order to test if protein levels were too low to visualize, another construct was made containing the *MIP1* gene under a copper inducible/repressible promoter, using the same pLK25 plasmid. Under the *CTR4* promoter DNA polymerase gamma can be overexpressed within the cell,⁷⁹ this will give an indication of whether the protein is being expressed highly enough to visualize, within the cell.

The KN99 mat α (Serotype A) strain of *C. neoformans* was transformed with the pLK25-*CTR4p-MIP1* plasmid in order to induce/repress expression of the MIP1 protein product along with an mCherry fusion protein. Cells containing this plasmid were treated with 200 μ m BCS and were imaged as described within the methods. Cells transformed with pLK25-*CTR4p-MIP1* showed very similar fluorescence to the cells transformed with pLK25-*MIP1*. A minority of transformed cells showed faint signal, indicating that some cells may contain the *MIP1*-mCherry fusion protein. This result suggested that low levels of protein expression were likely not the cause of low fluorescence within the pLK25-*MIP1* transformed cells. The low level of fluorescence present within transformed cells may be due to degradation of the protein, or that high levels of the polymerase are toxic within the cell. Western blots have not yet been performed to confirm the presence of the fusion protein in the cell. Due to the possibility of the mCherry protein being degraded within the cell, a new construct was designed using a GFP protein that had been codon optimized for expression within *C. neoformans*.

E. Future Directions

i. Localizing *MIP1* using *C. neoformans* codon optimized mEGFP

Due to failure of previous attempts to localize Cnp1G using an mCherry tag, a plasmid containing the *C. neoformans GPD* promoter upstream of the codon optimized EGFP gene have been obtained. In future this plasmid will continue to be used for the creation of a *MIP1*-GFP fusion protein that can be expressed within *C. neoformans*, and used to determine the *in vivo* localization of the corresponding protein. The use of a fluorescent protein that has been codon optimized for use within this organism should help create a fusion protein that will be stably maintained, and not degraded within the cell.

ii. Replacement of the endogenous promoter with the *CTR4* copper inducible promoter within the genome of *C. neoformans*

To further confirm the essentiality of *MIP1* within *C. neoformans* the endogenous *MIP1* promoter will be replaced with the *CTR4* copper inducible promoter within the genome. This will be carried out by creating a *CTR4p-MIP1*-mCherry construct that contains 3' and 5' sequence that is homologous to the surrounding genomic DNA in the cell. Using the homology of this construct to the surrounding area of the wild type gene, homologous recombination will be used to replace the endogenous *MIP1* gene along with its promoter within the cell. This will allow the expression of the *MIP1* gene *in vivo* to be effectively turned off, using the copper inducible promoter, effectively showing a *MIP1* knockout phenotype within *C. neoformans*. This experiment should further confirm the effect of *MIP1* depletion in *C. neoformans*.

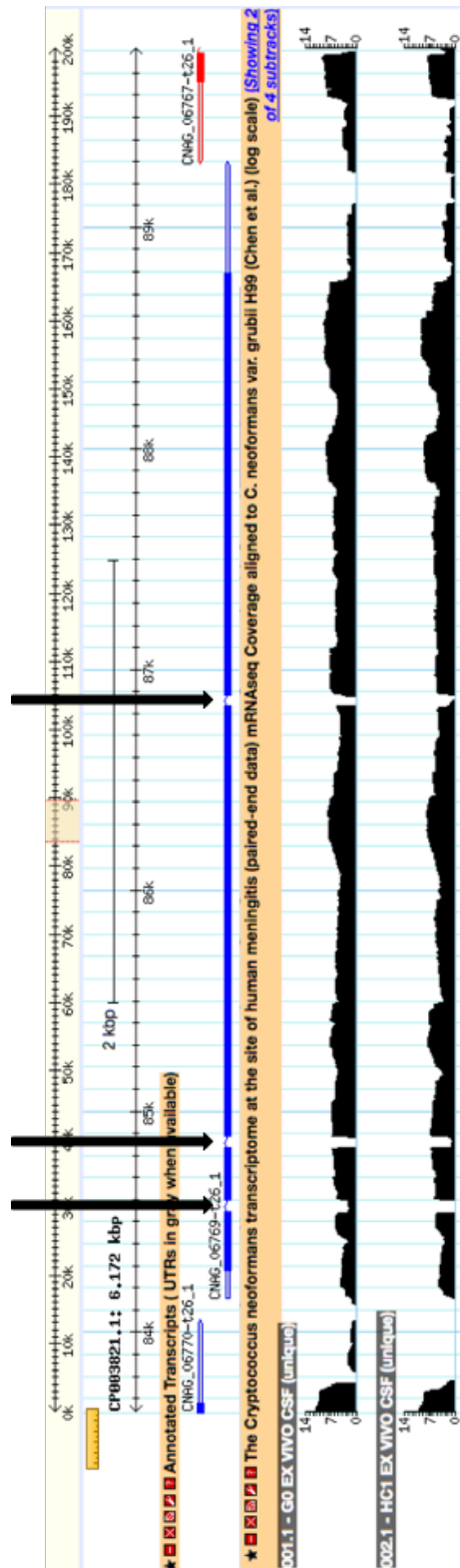


Figure 18. RNA seq data from multiple laboratories showing the production of mRNA from the CnMIP1 gene. This data was collected from FungiDB.com. Black arrows indicate introns within the CnMIP1 gene.

iii. Activity of CnpolG and study of its domains

Work is currently being carried out to determine the wild type activity of DNA polymerase gamma within *C. neoformans* (Wallen, direct communication). With the activity of the wild type protein established, biochemical techniques can be used to determine what role portions of the unknown regions within the protein play within the proper folding, or function of CnpolG. Due to the CnpolG enzyme containing a short c-terminal tail compared to ScpolG, it will be interesting to determine if the unknown domains function to bind accessory proteins that are needed for DNA synthesis, or repair. Biochemical studies involving specific deletions and even substitutions will reveal insight on how the protein functions within this organism, and what differences exist between the DNA polymerase gamma within *C. neoformans*, compared to those of *S. cerevisiae* or humans. If significant differences within the proteins can be discovered these regions could be used as potential drug targets for use in treatment of Cryptococcal meningoencephalitis in humans. Cheaper drugs with less detrimental side effects could possibly be designed using this information, allowing a more widespread availability to drugs of this nature.

A better understanding of the DNA polG protein could also assist with forming a better understanding of polG associated disease in humans. Many specific residues are currently known to be directly linked with specific diseases in humans, and more are sure to be identified in the future. Studies within yeast models could provide insight into potential disease associated regions that have not yet been studied within other higher eukaryotes.

REFERENCES

1. Webster J, Weber R. Introduction to Fungi, Third Edition.09/01/2007. Cambridge University Press.
2. Lengeler KB, Cox GM, Heitman J. 2001. Serotype AD Strains of *Cryptococcus neoformans* Are Diploid or Aneuploid and Are Heterozygous at the Mating-Type Locus. Petri WA, ed. *Infection and Immunity*. 69(1):115-122.
3. Callejas A, Ordonez N, Rodriguez MC, Castaneda E. 1998. First isolation of *Cryptococcus neoformans* var. *gattii*, serotype C, from the environment in Colombia. *Med. Mycol.* 36:341–44
4. Mamidi, A., DeSimone, J.A. & Pomerantz, R.J. 2002. Central nervous system infections in individuals with HIV-1 infection. *Journal of Neuro Virology*. 8: 158.
5. Del Valle L, Piña-Oviedo S. 2006. HIV disorders of the brain: pathology and pathogenesis. *Front Biosci*. 1; 11:718-732.
6. Kontoyiannis D, Peitsch W, Reddy B, Whimbey E, Han X, Bodey G, Rolston K. 2001. Cryptococcosis in Patients with Cancer. *Clinical Infectious Diseases*. Volume 32, Issue 11. 145-150.
7. Busse O. Uber parasitare Zelleinschlusse und ihre Zuchtung. *Centralbl. Bakt. Parasit.* 1894;16
8. Sanfelice F. Contributo alla morfologia e biologia dei blastomiceti che si sviluppano nei succhi de alcuni frutti. *Ann. Ist. Ig. R. Univ. Roma*. 1894; 4:463–469.
9. Barnett JA. A history of research on yeasts 14: medical yeasts part 2, *Cryptococcus neoformans*. *Yeast*. 2010; 27:875–904.
10. Bennett JE, Kwon-Chung KJ, Theodore TS. 1978. Biochemical differences between serotypes of *Cryptococcus neoformans*. *Sabouraudia* 16(3):167-74.
11. Kwon-Chung KJ. 1975. A new genus, *Filobasidiella*, the perfect state of *Cryptococcus neoformans*. *Mycologia*.67:1197–1200.

12. Know-Chung K. 1978. A new species of Filobasidella, the sexual state of *Cryptococcus neoformans* B and C serotypes. *Mycologia*. 68(4):943-6.
13. Bennett J E, Kwon-Chung K J, Howard D H. 1977. Epidemiologic differences among serotypes of *Cryptococcus neoformans*. *Am J Epidemiol*.105:582–586.
14. Dromer F, Mathoulin S, Dupont B, Letenneur L, Ronin O. 1996. Individual and environmental factors associated with infection due to *Cryptococcus neoformans* serotype D. *Clin. Infect Dis*. 23:91–96.
15. Martinez L, Garcia-Rivera, Casadevall A. 2001. *Cryptococcus neoformans* var. *neoformans* (Serotype D) Strains Are More Susceptible to Heat than *C. neoformans* var. *grubii* (Serotype A) Strains. *J Clin. Microbiol*. 39(9): 3365–3367.
16. Bolaños, B., and T. G. Mitchell. 1989. Phagocytosis of *Cryptococcus neoformans* by rat alveolar macrophages. *J. Med. Vet. Mycol*. 27:203-217.
17. Cherniak R, Sundstrom J. 1994. Polysaccharide antigens of the capsule of *Cryptococcus neoformans*. *Infection and Immunity*. 62(5):1507-1512.
18. Casadevall A. 2012. Amoeba Provide Insight into the Origin of Virulence in Pathogenic Fungi. In: Mylonakis E., Ausubel F., Gilmore M., Casadevall A. (eds) Recent Advances on Model Hosts. *Advances in Experimental Medicine and Biology*, vol 710. Springer, New York, NY
19. Chang, Y. C., and K. J. Kwon-Chung. 1994. Complementation of a capsule-deficient mutation of *Cryptococcus neoformans* restores its virulence. *Mol. Cell. Biol*. 14:4912-4919.
20. Kozel T. R. 1977. Non-encapsulated variant of *Cryptococcus neoformans*. II. Surface receptors for cryptococcal polysaccharide and their role in inhibition of phagocytosis by polysaccharide. *Infect. Immun*. 16, 99–106

21. Macher A, Bennett J, Gadek J, Frank M. 1978. Complement Depletion in Cryptococcal Sepsis. *The Journal of Immunology*. 120 (5) 1686-1690.
22. Kozel T, Gulley W, Cazin J. 1997. Immune response to *Cryptococcus neoformans* soluble polysaccharide: immunological unresponsiveness. *Infection and Immunity*. 18;3 701-707.
23. Nosanchuk J, Casadevall A. 1997. Cellular charge of *Cryptococcus neoformans*: contributions from the capsular polysaccharide, melanin, and monoclonal antibody binding. *Infection and immunity*. 65;5 1836-1841.
24. Vecchiarelli A, Retini C, Pietrella D, et al. 1995. Downregulation by cryptococcal polysaccharide of tumor necrosis factor alpha and interleukin-1 beta secretion from human monocytes. *Infection and Immunity*. 63(8):2919-2923.
25. Callejas A, Ordonez N, Rodriguez MC, Castaneda E. 1998. First isolation of *Cryptococcus neoformans* var. *gattii*, serotype C, from the environment in Colombia. *Med. Mycol*. 36:341-44
26. Missall T, Moran J, Corbett J, Lodge J. 2005. Distinct stress responses of two functional laccases in *Cryptococcus neoformans* are revealed in the absence of the thiol-specific antioxidant Tsa1. *Eukaryot. Cell*. 4:202-208.
27. 16. Zhu Xudong, Williamson P. 2004. Role of laccase in the biology and virulence of *Cryptococcus neoformans*. *FEMS Yeast Research*. 5;1. 1-10.
28. 76. Salas, S.D., Bennett, J.E., Kwon-Chung, K.J., Perfect, J.R., Williamson, P.R. 1996. Effect of the laccase gene *CNLAC1*, on virulence of *Cryptococcus neoformans*. *J. Exp. Med* 184, 377-386.
29. Wang Y, Casadevall A. 1995. *Cryptococcus neoformans* melanin and virulence: mechanism of action. *Infection and immunity*. 63;8 3131-3136.

30. Wang Y, Aisen P, Casadevall A. 1996. Melanin, melanin “ghosts,” and melanin composition in *Cryptococcus neoformans*. *Infection and immunity*. 64;7 2420-2424.
31. Nosanchuk J, Casadevall A. 1997. Cellular charge of *Cryptococcus neoformans*: contributions from the capsular polysaccharide, melanin, and monoclonal antibody binding. *Infection and immunity*, 65;5 1836-1841.
32. Rosas A, Casadevall A. 1997. Melanization affects susceptibility of *Cryptococcus neoformans* to heat and cold, *FEMS Microbiology Letters*, Volume 153, Issue 2, 1 Pages 265–272
33. Wang Y, Casadevall A. 1994. Growth of *Cryptococcus neoformans* in presence of L-dopa decreases its susceptibility to amphotericin B. *Antimicrob. Agents Chemother.* 38;11 2648-2650.
34. Cox, G. M, Cole G, Perfect J. Identification of and disruption of the *Cryptococcus neoformans* urease gene, abst 1.6:150. 3rd International Conference on *Cryptococcus* and Cryptococcosis, Paris.
35. Odom A, Muir S, Lim E, Toffaletti DL, Perfect J, Heitman J. 1997. Calcineurin is required for virulence of *Cryptococcus neoformans*. *The EMBO Journal*. 16(10):2576-2589.
36. Rodrigues M, Nakayasu E, Oliveira D, et al. 2008. Extracellular Vesicles Produced by *Cryptococcus neoformans* Contain Protein Components Associated with Virulence. *Eukaryotic Cell*. 7(1):58-67.
37. Brown, R. 1833. Observations on the organs and the mode of fecundation in Orchidae and Asclepiadeae. *Trans. Linn. Soc.* 16: 685-745
38. Altmann, R. 1890. Die Elementarorganismen und ihre Beziehungen zu den Zellen. Veit, Leipzig.

39. Benda C 1898. Ueber die spermatogenese der vertebraten und höherer evertebraten, II. Theil: Die histiogenese der spermien. Arch Anat Physiol 73: 393–398
40. Michaelis, L. 1900. Arch. Mikrosk. Anal. 55:558-575
41. Lazarow, A., and S. J. Cooperstein. 1953. J. Histochem. Cytochem.1:234-241
42. Meves, F. 1908. Arch. Mikrosk. Anal.72 :816-867
43. Regaud, C. 1909. C.R. Soc. Biol. 66:1034-1036.
44. Krebs, H.A., and W. A. Johnson. 1937. Biochem. J. 31 :645-660
45. Kalckar, H. 1937. Enzymologia. 2 :47-52.
46. Berg JM, Tymoczko JL, Stryer L. 2002. Biochemistry. 5th edition. New York: W H Freeman; Chapter 17, The Citric Acid Cycle. Available from:
47. Alberts B, Johnson A, Lewis J, et al. 2002. Molecular Biology of the Cell. 4th edition. New York: Garland Science. Electron-Transport Chains and Their Proton Pumps.
48. Berg JM, Tymoczko JL, Stryer L. Biochemistry. 5th edition. New York: W H Freeman; 2002. Section 16.1, Glycolysis Is an Energy-Conversion Pathway in Many Organisms.
49. Anderson S, Bankier A, Barrell B, Bruijn M, Coulson A, Drouin J. 1981. Sequence and organization of the human mitochondrial genome. Nature 290, 457-465.
50. Taanman J. 1999. The mitochondrial genome: structure, transcription, translation and replicaton. BBA, Bioenergetics. 1410, 2. 103-123.
51. Foury F. 1989. Cloning and sequencing of the nuclear gene *MIP1* encoding the catalytic subunit of the yeast mitochondrial DNA polymerase. J. Biol. Chem. 264, 20552–20560.
52. Wintersberger U, Wintersberger E. 1970. Studies on deoxyribonucleic acid polymerases from yeast. 2. Partial purification and characterization of mitochondrial DNA polymerase from wild type and respiration-deficient yeast cells. European Journal of Biochemistry. 13(1):20-27

53. Wintersberger, U., and Blutsch, H. 1976. DNA-dependent DNA polymerase from yeast mitochondria. Dependence of enzyme activity on conditions of cell growth, and properties of the highly purified polymerase. *Eur. J. Biochem.* 68, 199–207.
54. Garcia-Gomez, S. *et al.* 2013. PrimPol, an archaic primase/polymerase operating in human cells. *Mol Cell* 52, 541–553.
55. Genga A, Bianchi L, Foury F. 1986 A nuclear mutant of *Saccharomyces cerevisiae* deficient in mitochondrial DNA replication and polymerase activity. *Journal of Biological Chemistry.* 261, 9328-9332.
56. Nicole Hance, Mats I. Ekstrand, Aleksandra Trifunovic; 2005. Mitochondrial DNA polymerase gamma is essential for mammalian embryogenesis, *Human Molecular Genetics* 14;13: 1775–1783
57. Chan S, Copeland W. 2009. DNA polymerase gamma and mitochondrial disease: understanding the consequence of POLG mutations. *Biochem Biophys Acta.* 1787(5); 312-319.
58. Young M. J., Theriault S. S., Li M., Court D. A. 2006. The carboxyl-terminal extension on fungal mitochondrial DNA polymerases: identification of a critical region of the enzyme from *Saccharomyces cerevisiae*. *Yeast* 23, 101–116.
59. Hu J. P., Vanderstraeten S., Foury F. 1995. Isolation and characterization of ten mutator alleles of the mitochondrial DNA polymerase-encoding *MIP1* gene from *Saccharomyces cerevisiae*. *Gene* 160, 105–110.
60. Ropp P, Copeland W. Characterization of a new DNA polymerase from *Schizosaccharomyces pombe*: a probable homologue of the *Saccharomyces cerevisiae* DNA polymerase gamma. *Gene.* 7;165(1):103-7

61. Ropp P, Copeland W. 1996. Cloning and characterization of the human mitochondrial DNA polymerase, DNA polymerase gamma. *Genomics*. 15;36(3):449-458.
62. Ye F, Carrodeguas JA, Bogenhagen DF. 1996. The gamma subfamily of DNA polymerases: cloning of a developmentally regulated cDNA encoding *Xenopus laevis* mitochondrial DNA polymerase gamma. *Nucleic Acids Research*. 24(8):1481-1488.
63. Lewis D, Farr C, Want Y, Lagina A, Kaguni L. Catalytic Subunit of Mitochondrial DNA Polymerase from *Drosophila* Embryos Cloning, Bacterial Overexpression, and Biochemical Characterization. *JBC*. 271, 23389-23394.
64. Foury F., Vanderstraeten S. 1992. Yeast mitochondrial DNA mutators with deficient proofreading exonucleolytic activity. *EMBO J*. 11, 2717–2726.
65. Trifunovic A, Wredeberg A, Falkenberg M, et al. 2004. Premature ageing in mice expressing defective mitochondrial DNA polymerase. *Nature*. 429, 417-423.
66. Lee Y. S., Kennedy W. D., Yin Y. W. 2009. Structural insight into processive human mitochondrial DNA synthesis and disease-related polymerase mutations. *Cell* 139, 312–324.
67. Lim SE, Longley MJ, Copeland WC. 1999. The mitochondrial p55 accessory subunit of human DNA polymerase gamma enhances DNA binding, promotes processive DNA synthesis, and confers N-ethylmaleimide resistance. *J Biol Chem*. 274:38197–38203.
68. 97. Wernette C. M. Kaguni L. S. 1986. A Mitochondrial DNA Polymerase from Embryos of *Drosophila melanogaster*. *J. Biol. Chem*. 261:14764-14770
69. Viikov K., Väljamäe P., Sedman J. 2011. Yeast mitochondrial DNA polymerase is a highly processive single-subunit enzyme. *Mitochondrion* 11, 119–126.

70. Viikov K., Jasnovidova O., Tamm T., Sedman J. 2012. C-terminal extension of the yeast mitochondrial DNA polymerase determines the balance between synthesis and degradation. PLoS ONE 7:e33482.
71. Graziewicz M, Longley M, Copeland W. 2006. DNA Polymerase Gamma in Mitochondrial DNA Replication and Repair. Chem rev. 106, 383-405.
72. Maier D, Farr CL, Poeck B, et al. 2001. Mitochondrial Single-stranded DNA-binding Protein Is Required for Mitochondrial DNA Replication and Development in *Drosophila melanogaster*. Fox TD, ed. *Molecular Biology of the Cell*. 12(4):821-830.
73. Maier D, Farr CL, Poeck B, et al. 2001. Mitochondrial Single-stranded DNA-binding Protein Is Required for Mitochondrial DNA Replication and Development in *Drosophila melanogaster*. Fox TD, ed. *Molecular Biology of the Cell*. 12(4):821-830.
74. Tyynismaa H, Sembongi H, Brown M, et al. 2004. Twinkle helicase is essential for mtDNA maintenance and regulates mtDNA copy number. *Human Molecular Genetics*. 13;24 3219-3227.
75. Cerritelli S, Frolova E, Feng C, Grinberg A, Love P, Crouch R. 2003. Failure to Produce Mitochondrial DNA Results in Embryonic Lethality in Rnaseh1 Null Mice. *Molecular Cell*. 11;3 807-815.
76. Bose I, Doering T. 2011. Efficient implementation of RNA interference in the pathogenic yeast *Cryptococcus neoformans*. *J Microbiol Methods*. 86(2):156-15.
77. Zhang H, Barceló JM, Lee B, et al. 2001. Human mitochondrial topoisomerase I. *Proceedings of the National Academy of Sciences of the United States of America*. 98(19):10608-10613.

78. Li M.Z., Elledge S.J. 2012. SLIC: A Method for Sequence- and Ligation-Independent Cloning. In: Peccoud J. (eds) Gene Synthesis. Methods in Molecular Biology (Methods and Protocols), vol 852. Humana Press
79. Ory, J. J., Griffith, C. L. and Doering, T. L. 2004. An efficiently regulated promoter system for *Cryptococcus neoformans* utilizing the *CTR4* promoter. *Yeast*, 21: 919–926.
80. Dougherty, R. (2005), "Extensions of DAMAS and Benefits and Limitations of Deconvolution in Beamforming", 11th AIAA/CEAS Aeroacoustics Conference (26th AIAA Aeroacoustics Conference).
81. Lodi T, Dallabona C, Nolli C, Goffrini P, Donnini C, Baruffini E. 2015. DNA polymerase gamma and disease: what we have learned from yeast. *Front Genet.* 6: 106.
82. Kwon-Chung KJ, Varma A, Edman JC, Bennett JE. 1992. Selection of *ura5* and *ura3* mutants from the two varieties of *Cryptococcus neoformans* on 5-fluorouracil acid medium. *J Med Vet Mycol.* 30(1):61-9.
83. Hong L, Cottrell T, Pierini L, Goldman W, Doering T. 2002. RNA Interference in the Pathogenic Fungus *Cryptococcus neoformans*. *Genetics* 160(2):463-470.
84. Lin X, Heitman J. 2006. The Biology of the *Cryptococcus neoformans* Species Complex. *Annu. Rev. Microbiol.* 60:69-105.

APPENDIX

S.
 C. MRKALDISRLTRPARIRCRPSLFLRNRSLSSASQSKPSDAPVKISDGKEEGVGKPLIPA

S.
 C. FGARRAEMEDYILAMEMAKLEDGYGQPRVRKIRKSKLPSLHDPQSFLCDSTQASSSKVTS

S. 1 10 20 30 40
 C. SASPTSQPSPKRGKELVVSNDYATNV.PNQDVQT.LEDAKPIDSGQSKSGPRRNPVGIQY

S. 50 60 70 80 90 100
 C. LSSSLHSQLEEG...QLPKPPQALLDISKRLKDNDFELEGAAVLPETSPNLPSSRGN

S. 110 120 130 140 150 160
 C. IRDHFQKTRFNSEPKSFCEDKFF.EEMVLRPAEW.LRKPGWVXYVPGM.APEVAVYVDE

S. 170 180 190 200
 C. ELVVDVEIYNSDIPITATALESRAWYEWCSPEFCGGDDPA.....

S. 210 220 230 240 250 260
 C. .ALTPL.NTINKEQVITGHNVYDRARVLEEYVFRDQSKAF.LDTQSLHVASPGICRQR

S. 270 280 290
 C. PMFMKNNKKKAEVSEV.....HPEISIDYDDPWL

S. 300 310 320 330 340 350
 C. NVSALNSLKKVAKFCIDDKDTRDFASTD...KSTIENFQKLVNYCATDVTATASQV

S. 360 370 380 390 400 410
 C. FDEIFPVLKCKCPHPVSFACDKSLSKCILETKLNDVYNSSESLVQOSKVVQTESKIVQ

S. 420 430 440 450
 C. IIKDIVLKRDKPDPYLYKDPWDSQIDWITKPLRLTKKGVPAKC.....Q

S. 460 470 480 490 500 510
 C. KLPGFPEWYRQLFPKSDTVEPKITIKSRILPILFKESWENSPIVWSKESGWCFNVPHEQV

S. 520 530
 ETYKAKNYVLA...DSV...QE...R...
 C. GDFDTHGSPHMLSAKDRLEKLE...R...

S.
 C. YPELLVKVMKTDLNDVVEDLWECVVDMGNLKESEWGQQLDWTPTTQDITSSNDVPLFSS

S. 540
 C. ...THN...

S. ...
 C. SSLRPSSIKKSKANLGIWPKWYDLDLTPVSRPLVGE...

S. 550 560
 C. ...CCTGV...

S. 570 580 590 600 610
 C. ...LAHQALQINS...

S. 620 630 640 650 660 670
 C. ...NDLAI...

S. 680 690 700 710 720 730
 C. ...GADVDSEELWI...

S. 740 750 760 770 780 790
 C. ...AKVFNYSRIYGAG...

S. 800 810 820 830 840
 C. ...GGSSEYLFN...

S. 850 860 870 880 890 900
 C. ...SMEYIKKYN...

S. 910 920 930 940 950 960
 C. ...AMALQISNIWTRAM...

S. 970 980 990 1000 1010 1020
 C. ...GALDINQLL...

```

      1030      1040      1050      1060      1070      1080
S.  MGVQSDKRDVNRLEDEYI RECTSKEYARDGNTAEYSLDDYI KDV EK KRTKVRIMG.SNF
C.  AQA S KGGMG...AKKID.....NLPPVQDSEVNECNEKPYQXSHKAV

      1090      1100      1110      1120      1130      1140
S.  TDGFKNAKADQRIRLPVNMPDYPTLHKIANDSAIPEKQLLENRRKKENRIDDENKKKLTR
C.  TSSSKKFQ.....

      1150      1160      1170      1180      1190      1200
S.  KKNTTPMERKYKRVYGGRKAFEFYECANKPLDYTLETEKQFFNIPIDGVIDDVLNDKSN
C.  .....

      1210      1220      1230      1240      1250
S.  YKKKPSQARTASSSPIRKKTAKAVHSKKLPARKSSTTNRNLVELERDITISREY
C.  .....

```

Figure 19. (S1). Protein alignment of *S. cerevisiae* polG and *C. neoformans* polG homolog.

	1	10	20	30	40	50	60
JEC21	MRKALDISRLTRPARIRCRPSLFLRMGSLSSASQSKPSDAPVKVSDVREKQVEKPLVPA						
H99	MRKALDISRLTRPARIRCRPSLFLRMRLSSASQSKPSDAPVKVSDVREKQVEKPLVPA						
	70	80	90	100	110	120	
JEC21	FGARRAEMEDIYLAMEMAKLEDGYDQPRVVKIRKSKLPSLHDPQSFLNDSKQASSSVTS						
H99	FGARRAEMEDIYLAMEMAKLEDGYDQPRVVKIRKSKLPSLHDPQSFLNDSKQASSSVTS						
	130	140	150	160	170	180	
JEC21	SASPTLQPSRKQKEKEVVAHSEYETSEPNQEVQTLQDAKPIDSEGRKSPRRNPVGVQMLS						
H99	SASPTLQPSRKQKEKEVVAHSEYATNVNQEVQTLQDAKPIDSEGRKSPRRNPVGVQMLS						
	190	200	210	220	230	240	
JEC21	SLHSQLFFGQPLPKPPQALLDISKSLKDNDFPEGAAVLPEISFLPSLRLGNNIRDF						
H99	SLHSQLFFGQPLPKPPQALLDISKSLKDNDFPEGAAVLPEISFLPSLRLGNNIRDF						
	250	260	270	280	290	300	
JEC21	RLGQYTAEPASMARFAATLPAKPRWEMGRSGWTKYISDGRMEAVDDLQDETIVSF						
H99	RLGQYTAEPASMARFAATLPAKPRWEMGRSGWTKYISDGRMEAVDDLQDETIVSF						
	310	320	330	340	350	360	
JEC21	DVEVLYKLSRFPVMAFAVTPNAWYSWLSPVIFQSPFAEIPKPLPPWEASIPTYHPNELIP						
H99	DVEVLYKLSRFPVMAFAVTPNAWYSWLSPVIFQSPFAEIPKPLPPWEASIPTYHPNELIP						
	370	380	390	400	410	420	
JEC21	LFNNKSSIPRIVIGHNVGYDRARVKEYSHERTQTRWLDTLSLHVSTRGITSVORPANMA						
H99	LFNNKSSIPRIVIGHNVGYDRARVKEYSHERTQTRWLDTLSLHVSTRGITSVORPANMA						
	430	440	450	460	470	480	
JEC21	YKKNKKAKKLREQENLSILOEMAESGDGTIMDGLQEFGAASETEAEALQSRWEDVTSM						
H99	YKKNKKAKKLREQENLSILOEMAESGDGTIMDGLQEFGAASETEAEALQSRWEDVTSM						
	490	500	510	520	530	540	
JEC21	NSLAEVAALHCGYPVDKSVDRFGDDSIKASQIHSELEQLLSYCADDVVRTHDVYAKVF						
H99	NSLAEVAALHCGYPVDKSVDRFGDDSIKASQIHSELEQLLSYCADDVVRTHDVYAKVF						
	550	560	570	580	590	600	
JEC21	PLFLESCPHPATLSCGLSMGSSFLPVDQSWKEYLNAEETTYREMDVAVKALRLLAEKLR						
H99	PLFLESCPHPATLSCGLSMGSSFLPVDQSWKEYLNAEETTYREMDVAVKALRLLAEKLR						
	610	620	630	640	650	660	
JEC21	AEGEPKRGDPWASQLDWSPKNARWSDLEDLCTGKHSYQPRESAQPKKPFNSGASSPFWL						
H99	AEGEPKRGDPWASQLDWSPKNARWSDLEDLCTGKHSYQPRESAQPKKPFNSGASSPFWL						

670 680 690 700 710 720
JEC21 TQISSNHSILKSNMSQRYLLPLLRMSFKGHPVAYLSEHGWCFTMVPHDQVGDYFDTHGSP
H99 TQISSNHSILKSNMSQRYLLPLLRMSFKGHPVAYLSEHGWCFTMVPHDQVGDYFDTHGSP

730 740 750 760 770 780
JEC21 HMLSAKDNRLKLEESYSFFRIGNAGSPKKTTLVGPSTKPFVNSGDLTSAYPELLIKVMK
H99 HMLSAKDSRLKLEESYSFFRIGNAGSPKKTTLVGPSTKPFVNSGDLTSAYPELLIKVMK

790 800 810 820 830 840
JEC21 TDLSDAVEDLWECVVDIGNLKESEWGQQLDWTFTTEGSASSNDVPLSSSSSSLRPSSIKK
H99 TDLNDVVEDLWECVVDIGNLKESEWGQQLDWTFTTQDITSSNDVPLSSSSSSLRPSSIKK

850 860 870 880 890 900
JEC21 SKTNHCITWPKNYWDLTGPVSRPLVGEGLDLCRRTIAPLLLRLLQWQQFPLVSKKELWLYR
H99 SKANLCITWPKNYWDLTGPVSRPLVGEGLDLCRRTIAPLLLRLLQWQQFPLVSKKELWLYR

910 920 930 940 950 960
JEC21 LPRKVVYEDERIAKARGLPVSPREEGPDAVFAKDDDHVYFRLPHKDGEGKXVGNPLSKG
H99 LPRKVVYEDERIAKARGLPVSPREEGPDAVFAKDDDHVYFRLPHKDGEGKXVGNPLSKG

970 980 990 1000 1010 1020
JEC21 FVKATIESGELASAAAESGDDVAAKAAADATNMNAFCSTWISSRERIMDQMVVYRDQEFQM
H99 FVKATIESGELASAAAESGDDVAAKAAADATNMNAFCSTWISSRERIMDQMVVYRDQEFQM

1030 1040 1050 1060 1070 1080
JEC21 ILPQVITMGTVTRRAVEATWLTASNAKNVRVGSSELKAMVRAPPGYSIVGSDVDSSELWIS
H99 ILPQVITMGTVTRRAVEATWLTASNAKNVRVGSSELKAMVRAPPGYSIVGSDVDSSELWIS

1090 1100 1110 1120 1130 1140
JEC21 SVMGDSQFGMHGATAIGWMTLEGKKSAGTDLHSKTAHILGISRDAAKVFNYSRIYAGKK
H99 SVMGDSQFGMHGATAIGWMTLEGKKSAGTDLHSKTAHILGISRDAAKVFNYSRIYAGKK

1150 1160 1170 1180 1190 1200
JEC21 HAVQLLQGDSEKLTKETAGKLADNLYKSTKGAKAVRARNLPVASEPDLWHGGSESYLFNT
H99 HAVQLLQGDSEKLTKETAGKLADNLYKSTKGAKAVRARNLPVASEPDLWHGGSESYLFNT

	1210	1220	1230	1240	1250	1260
JEC21	LEAIALSDRPTTPALGCGVTRALRKSYLEEASYLPSRVNWWWQSSQVDYLHLLIVSMEY					
H99	LEAIALSDRPTTPALGCGVTRALRKSYLEEASYLPSRVNWWWQSSQVDYLHLLIVSMEY					
	1270	1280	1290	1300	1310	1320
JEC21	LIKKYDIFARYLISVHDEVRYLAKEEDRYRTALALQANAWTRALFCFNLGIDDMPQGIT					
H99	LIKKYNIQARYLISVHDEVRYLAKEEDRYRTALALQANAWTRALFCFNLGIDDMPQGIT					
	1330	1340	1350	1360	1370	1380
JEC21	FFSAVDIDHVLRKEVFLTCETPSHPKVIPAGESLDINSLLEKIPRODLGTFIPDDLQPTT					
H99	FFSAVDIDHVLRKEVFLTCETPSHPKVIPAGESLDINSLLEKIPRODLGTFIPDDLQPTT					
	1390	1400	1410	1420	1430	1440
JEC21	DIKPPVALFPNIQSAQHRQFLQAQASKGGMGARKWLDNLPVQYIDEVNEENIKPKYQKSH					
H99	DIKPPVALFPNIQSAQHRQFLQAQASKGGMGARKWLDNLPVQYIDEVNEENIKPKYQKSH					
	1450					
JEC21	KKAVLSSSKK.					
H99	KKAVLSSSKK.					

Figure 20. (S2). Protein alignment of JEC21 (Serotype D) (top) and H99 (Serotype A) (bottom) *C. neoformans* DNA polymerase gamma.